Studies on the effect of marine carotenoid, astaxanthin, on age-related diseases which caused by mitochondrial dysfunction

ミトコンドリア機能不全による加齢性疾患に対する
海洋性カロテノイド類アスタキサンチンの効果に関する研究

February 2023

Graduate School of Fisheries and Environmental Sciences

Nagasaki University

長崎大学大学院水産・環境科学総合研究科

Luchuanyang Sun

Contents

Chapter I General introduction

1.1 Aging and age-related diseases

The aging of the population is the inevitability of socio-economic development and scientific and technological progress. Worldwide, the proportion of people over 65 years of age in the total population (the rate of advanced ageing) is growing rapidly (Figure 1-1), especially in China and Japan (Figure 1-2). The aging of the population is a major global issue in the 21st century, and it is also a key issue that must be faced and resolved in global social and economic development.

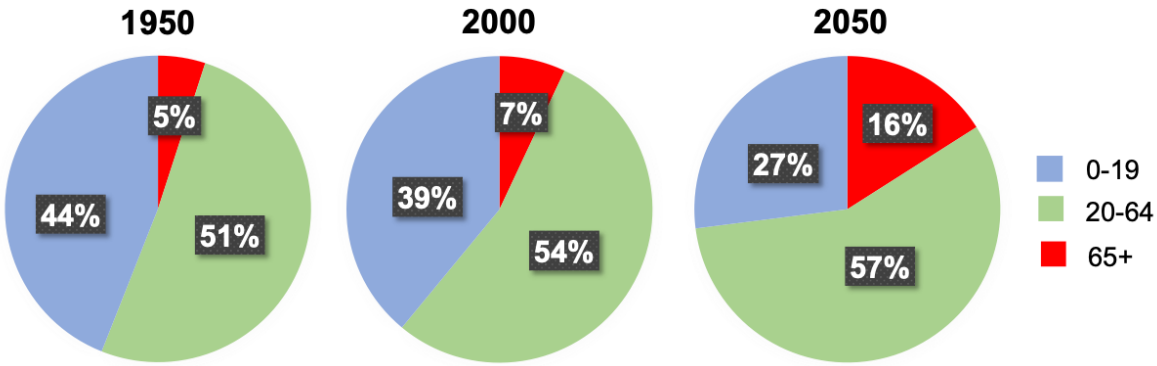

Source: http://study-aids.co.uk/dissertation-blog/population-ageing/

Figure 1-1. The proportion of the global population as relates to age

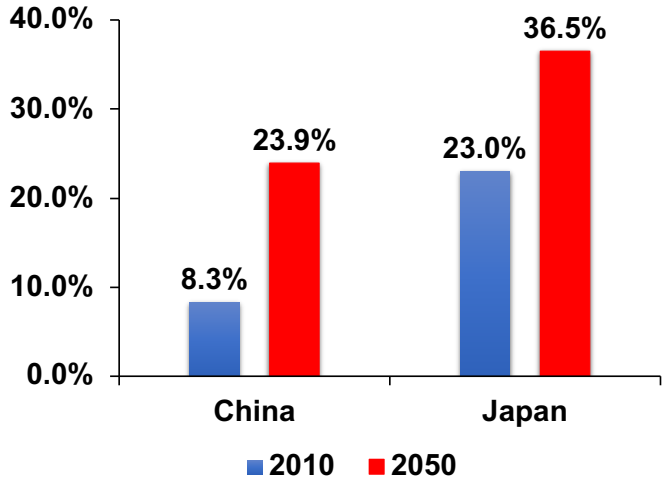

Source:
United Nations, Department of Economic and Social Affairs, World population Prospects, 2013

Figure 1-2. Population of people 65+ in China and Japan (%) estimates for 2010 and 2050

Aging is a complex biological process characterized by functional decline of tissues and organs, structural degradation, reduced adaptability and resistance, leading to increased morbidity and mortality [1]. This complex biological process involves the damage of many cellular organelles, such as mitochondria, endoplasmic reticulum, and the alteration in biological process including energy metabolism, biosynthesis, which reducing cell proliferation and causing cellular senescence.

As aging progresses, it increases the incidence to diseases associated with this process, such as atherosclerosis (cardiovascular disease) [2], diabetes (metabolic disorders) [3], sarcopenia (muscle aging and dysfunction) [4], Alzheimer's diseases (brain aging and neurodegenerative disease) [5], macular degeneration (eye disease) [6], and so on. Age-related diseases pose a serious threat to human health and reduce the quality of life of the elderly.

Hence, how to elucidate the mechanism of aging, delay the aging process, reduce the occurrence of age-related diseases, and maintain an unfading appearance during the aging process has become a global topic and problem [7].

1.2 The role of mitochondria in aging

Mitochondria are usually referred to as the powerhouse of the cell. They help turn the energy we take from food into energy that the cell can use. Metabolites are oxidized through the tricarboxylic acid (TCA) cycle in the mitochondrial matrix and then pass through the electron transport chain (ETC) in the inner membrane of mitochondria to produce adenosine-triphosphate (ATP). In addition to the production of ATP, mitochondria play an important role in a variety of other cellular processes, such as apoptosis, β-oxidation of fatty acids, and iron-sulfur cluster synthesis [8]. However, as cells and organisms age, the efficacy of the respiratory chain trends to diminish, thus increasing electron leakage and reducing ATP generation [9]. Moreover, with age, mitochondria display changes in morphology, abundance, and oxidative phosphorylation (OXPHOS) activity [10]. The relationship between mitochondrial dysfunction and aging has been long discussed.

In the sophisticated mechanism of aging, one of the accepted theories is the mitochondrial free radical theory. This theory raised that mitochondrial dysfunction occurs with the progression of aging, induces to the increased production of ROS, which in turn results in further mitochondrial deterioration and global cellular damage [11]. Similarly, mitochondrial aging theory (improved version of the mitochondrial free radical theory) was proposed [12]. Briefly, both theories considered that with the increase of age, cellular senescence are caused

by excessive ROS production [13]. Although the accumulation of oxidative damage occurs with age, how intracellar ROS or mitochondrial ROS directly or indirectly affects aging remains controversial.

Additionally, dysfunctional mitochondria can lead to aging independently of ROS [14, 15]. This could happen through variety number of mechanisms, many reports indicate these mechanisms appear to be involved in mitochondrial integrity and biogenesis [1]. On one hand, mitochondrial deficiencies may affect apoptotic signaling by increasing the propensity of mitochondria to permeabilize in response to stress [16]. Also, mitochondrial dysfunction may directly impact cellular signaling and intraorganellar crosstalk by affecting the interface between the outer mitochondrial membrane and the endoplasmic reticulum [17]. On the other hand, the efficiency of mitochondrial bioenergetics decreases with age, possibly due to multiple aggregation mechanisms, including reduced mitochondrial biogenesis. For instance, the depletion of telomere in p53-null mice have normal PGC-1α and PGC-1β expressions, increased mitochondrial DNA content [18]. However, this mitochondrial decline can be reversed by telomerase activation in wild-type mice during physiological aging [19]. Other mechanisms causing defective bioenergetics include accumulation of DNA mutations, destabilization of the mitochondrial complexes, varies in the lipid composition of mitochondrial membranes, alterations in mitochondrial dynamics (imbalance of fission and fusion), and the defectively quality control by mitophagy [1]. Totally, the increased damage in mitochondria, caused by lower biogenesis and reduced clearance, may contribute to and accelerate the aging process.

Although severe mitochondrial dysfunction is pathogenic, mild respiratory dysfunction may extend lifespan [20]. Metformin and resveratrol are mild mitochondrial poisons that induce a low energy state characterized by increased adenosine 5'-monophosphate-activated protein kinase (AMPK) levels and activation of AMPK [21]. Interestingly, recent studies have also shown that metformin delays worm aging by impairing folate and methionine metabolism in the worm gut microbiome [22]. Moreover, metformin increases lifespan in mice if taken from early life. Likewise, even though resveratrol does not extend mice lifespan under normal dietary condition [23, 24], the co-intake of resveratrol and sirtuin activator SRT1720 protect mice from metabolic damage and improve mitochondrial respiration in a PGC-1α-dependent manner [25, 26].

Over the past few decades, multiple lines of evidence in model organisms and humans have shown that mitochondrial function has a profound impact on the aging process. Mitochondrial dysfunction contributes to age-related disease phenotypes and aging. Therefore, targeting mitochondria to slow aging and age-related diseases has become a point of interest.

1.3 Astaxanthin (AX), a marine carotenoid with stronger antioxidant activity

Astaxanthin (AX; 3,3'-dihydroxy-β, β'-carotene-4,4'-dione) is widely known as a potent antioxidant. It is a kind of carotenoid with long conjugated double bonds, keto groups, and hydroxyl groups (Figure 1-3). AX has the molecular formula $C_{40}H_{52}O_4$. Its molar mass is 596.84 g/mol. AX naturally accumulates in algae, yeast, salmon, crustaceans, fish epidermis, and other biologicals [27, 28]. Main sources of AX such as *Haematococcus pluvialis*, wild caught salmon, yeast and their content are shown in Table 1-1. The United States Food and Drug

Administration (USFDA) has approved the use of AX as food colorant in animal and fish feed [29]. The European Commission considers natural AX as a food dye [30].

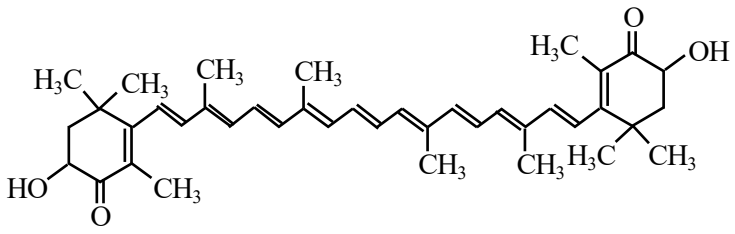

Figure 1-3. Structure of Astaxanthin

Table 1-1. Main sources and contents of AX

Source	Content (mg/kg)
Haematococcus pluvialis	10,000~25,000
Phaffia	2,000~8,000
Socheye salmon	30~58
Coho salmon	9~28
Atlantic salmon	5~7
Pink salmon	3~7
Chum salmon	1~8

In the past, the different bioactivities have been investigated in AX such as anti-oxidant [31-37], anti-inflammation [38, 39], anti-diabet [40, 41], anti-tumor [42, 43], prevention of cardiovascular disease [44, 45], and immunity regulatory [46, 47]. The unique molecular structure of AX allows for its insertion through the lipid bilayer of cell membranes, leading to stronger protection against oxidative stress and free-radical-scavenging effects at the cell membrane than other antioxidants such as β-carotene, α-tocopherol, and vitamin C [28]. Interestingly, it was reported that AX appears to aggregate more readily in organelles containing bilayer membrane structures, such as mitochondria [48]. AX reportedly maintains mitochondrial integrity by reducing oxidative stress, prevents the loss of mitochondrial membrane potential, and increases mitochondrial oxygen consumption, which inhibits mitochondrial dysfunction [49-51]. Additionally, AX suppresses bleomycin-induced ROS generation and apoptosis mediated by the disturbed mitochondrial signaling pathway in type II alveolar epithelial cells [52]. These reports raise the possibility that AX acts in both the mitochondrial and cell membranes. Therefore, AX is being studied for mitochondria-related diseases due to its unique structure and activity.

1.4 Objective

In this study, the objective is to investigate the effect of AX on age-related diseases which caused by mitochondrial dysfunction. In Chapter II, the effect of AX on skeletal muscle atrophy was investigated. Muscle atrophy model was established by tail-suspension in C57BL/6J mice. An AX-supplemented diet was fed to mice. Morphological analysis, intramuscular mitochondrial protein and genetic analysis were conducted to estimate the effect of AX. The

mechanisms of AX action on muscle atrophy were explored by Sol8 myotubes modeling. In Chapter III, the effect of AX on immune disorder was investigated. Inflammation was established by the classical model of LPS stimulation of RAW264.7 cells. The effects of AX on inflammation and the unique mechanisms of AX targeting mitochondria to regulate immunity were investigated by measuring the expression and release of cytokines, mitochondrial function indicators, the activity and expression level of important metabolic enzymes in mitochondria, and the migration of mitochondrial energy metabolism. In Chapter IV, the role of AX in two typical age-related diseases caused by mitochondrial dysfunction and the mechanisms of protective effects of AX on mitochondrial function were summarized and discussed. The potent regulation role of AX in other age-related diseases due to mitochondrial dysfunction and metabolic disorders was prospected.

1.5 References

[1] López-Otín, C.; Blasco MA, Partridge L, Serrano M, Kroemer G. The hallmarks of aging. *Cell* 2013, *153*, 1194-217.

[2] Wang, J.C.; Bennett, M. Aging and atherosclerosis: mechanisms, functional consequences, and potential therapeutics for cellular senescence. *Circ. Res*. 2012, *111*, 245-59.

[3] Bloomgarden, Z.; Ning, G. Diabetes and aging. *J. Diabetes* 2013, *5*, 369-71.

[4] Dao, T.; Green, A.E.; Kim, Y.A.; Bae, S.J.; Ha, K.T.; Gariani, K.; Lee, M.R.; Menzies, K.J.; Ryu, D. Sarcopenia and Muscle Aging: A Brief Overview. *Endocrinol Metab. (Seoul)* 2020, *35*, 716-732.

[5] Baker, D.J.; Petersen, R.C. Cellular senescence in brain aging and neurodegenerative diseases: evidence and perspectives. *J. Clin. Invest.* 2018, *128*, 1208-1216.

[6] Gheorghe, A.; Mahdi, L.; Musat, O. AGE-RELATED MACULAR DEGENERATION. *Rom. J. Ophthalmol.* 2015, *59*, 74-7.

[7] Liu, Y.; Weng, W.; Gao, R.; Liu, Y. New Insights for Cellular and Molecular Mechanisms of Aging and Aging-Related Diseases: Herbal Medicine as Potential Therapeutic Approach. *Oxid. Med. Cell Longev*. 2019, 4598167.

[8] Kauppila, T.E.S.; Kauppila, J.H.K.; Larsson, N.G. Mammalian Mitochondria and Aging: An Update. *Cell Metab.* 2017, *25*, 57-71.

[9] Hekimi, S.; Lapointe, J.; Wen, Y. Taking a "good" look at free radicals in the aging process. *Trends Cell Biol.* 2011, *21*, 569-76.

[10] Shigenaga, M.K.; Hagen, T.M.; Ames, B.N. Oxidative damage and mitochondrial decay in aging. *Proc. Natl. Acad. Sci. U. S. A.* 1994, *91*, 10771-8.

[11] Harman, D. Aging: a theory based on free radical and radiation chemistry. *J. Gerontol.* 1956, *11*, 298-300.

[12] Alexeyev, M.F. Is there more to aging than mitochondrial DNA and reactive oxygen species? *FEBS. J.* 2009, *276*, 5768-87.

[13] Kauppila, T.E.S.; Kauppila, J.H.K.; Larsson, N.G. Mammalian Mitochondria and Aging: An Update. *Cell Metab.* 2017, *25*, 57-71.

[14] Edgar, D.; Shabalina, I.; Camara, Y.; Wredenberg, A.; Calvaruso, M.A.; Nijtmans, L.; Nedergaard, J.; Cannon, B.; Larsson, N.G.; Trifunovic, A. Random point mutations with major effects on protein-coding genes are the driving force behind premature aging in mtDNA mutator mice. *Cell Metab.* 2009, *10*, 131-8.

[15] Hiona, A.; Sanz, A.; Kujoth, G.C.; Pamplona, R.; Seo, A.Y.; Hofer, T.; Someya, S.; Miyakawa, T.; Nakayama, C.; Samhan-Arias, A.K.; Servais, S.; Barger, J.L.; Portero-Otín, M.; Tanokura, M.; Prolla, T.A.; Leeuwenburgh, C. Mitochondrial DNA mutations induce mitochondrial dysfunction, apoptosis and sarcopenia in skeletal muscle of mitochondrial DNA mutator mice. *PLoS One.* 2010, *5*, e11468.

[16] Kroemer, G.; Galluzzi, L.; Brenner, C. Mitochondrial membrane permeabilization in cell death. *Physiol. Rev.* 2007, *87*, 99-163.

[17] Raffaello, A.; Rizzuto, R. Mitochondrial longevity pathways. *Biochim. Biophys. Acta.* 2011, *1813*, 260-8.

[18] Sahin, E.; DePinho, R.A. Axis of ageing: telomeres, p53 and mitochondria. *Nat. Rev. Mol. Cell Biol.* 2012, *13*, 397-404.

[19] Bernardes de Jesus, B.; Vera, E.; Schneeberger, K.; Tejera, A.M.; Ayuso, E.; Bosch, F.; Blasco, M.A. Telomerase gene therapy in adult and old mice delays aging and increases longevity without increasing cancer. *EMBO. Mol. Med.* 2012, *4*, 691-704.

[20] Haigis, M.C.; Yankner, B.A. The aging stress response. *Mol. Cell* 2010, *40*, 333-44.

[21] Hawley, S.A.; Ross, F.A.; Chevtzoff, C.; Green, K.A.; Evans, A.; Fogarty, S.; Towler, M.C.; Brown, L.J.; Ogunbayo, O.A.; Evans, A.M.; Hardie, D.G. Use of cells expressing gamma subunit variants to identify diverse mechanisms of AMPK activation. *Cell Metab.* 2010, *11*, 554-65.

[22] Cabreiro, F.; Au, C.; Leung, K.Y.; Vergara-Irigaray, N.; Cochemé, H.M.; Noori, T.; Weinkove, D.; Schuster, E.; Greene, N.D.; Gems, D. Metformin retards aging in C. elegans by altering microbial folate and methionine metabolism. *Cell* 2013, *153*, 228-39.

[23] Pearson, K.J.; Baur, J.A.; Lewis, K.N.; Peshkin, L.; Price, N.L.; Labinskyy, N.; Swindell, W.R.; Kamara, D.; Minor, R.K.; Perez, E.; Jamieson, H.A.; Zhang, Y.; Dunn, S.R.; Sharma, K.; Pleshko, N.; Woollett, L.A.; Csiszar, A.; Ikeno, Y.; Le Couteur, D.; Elliott, P.J.; Becker, K.G.; Navas, P.; Ingram, D.K.; Wolf, N.S.; Ungvari, Z.; Sinclair, D.A.; de Cabo, R. Resveratrol delays age-related deterioration and mimics transcriptional aspects of dietary restriction without extending life span. *Cell Metab.* 2008, *8*, 157-68.

[24] Strong, R.; Miller, R.A.; Astle, C.M.; Baur, J.A.; de Cabo, R.; Fernandez, E.; Guo, W.; Javors, M.; Kirkland, J.L.; Nelson, J.F.; Sinclair, D.A.; Teter, B.; Williams, D.; Zaveri, N.; Nadon, N.L.; Harrison, D.E. Evaluation of resveratrol, green tea extract, curcumin, oxaloacetic acid, and medium-chain triglyceride oil on life span of genetically heterogeneous mice. *J. Gerontol. A. Biol. Sci. Med. Sci.* 2013, *68*, 6-16.

[25] Feige, J.N.; Lagouge, M.; Canto, C.; Strehle, A.; Houten, S.M.; Milne, J.C.; Lambert, P.D.; Mataki, C.; Elliott, P.J.; Auwerx, J. Specific SIRT1 activation mimics low energy levels and protects against diet-induced metabolic disorders by enhancing fat oxidation. *Cell Metab.* 2008, *8*, 347-58.

[26] Minor, R.K.; Baur, J.A.; Gomes, A.P.; Ward, T.M.; Csiszar, A.; Mercken, E.M.; Abdelmohsen, K.; Shin, Y.K.; Canto, C.; Scheibye-Knudsen, M.; Krawczyk, M.; Irusta, P.M.; Martín-Montalvo, A.; Hubbard, B.P.; Zhang, Y.; Lehrmann, E.; White, A.A.; Price, N.L.; Swindell, W.R.; Pearson, K.J.; Becker, K.G. Bohr, V.A. Gorospe, M.; Egan, J.M.; Talan, M.I.; Auwerx, J. Westphal, C.H.; Ellis, J.L.; Ungvari, Z.; Vlasuk, G.P.; Elliott, P.J.; Sinclair, D.A.; de Cabo, R. SRT1720 improves survival and healthspan of obese mice. *Sci. Rep.* 2011, *1*, 70.

[27] Yuan, J.P.; Peng, J.; Yin, K.; Wang, J.H. Potential health-promoting effects of astaxanthin: A high-value carotenoid mostly from microalgae. *Mol. Nutr. Food Res.* 2011, *55*, 150-165.

[28] Ambati, R.R.; Phang, S.M.; Ravi, S.; Aswathanarayana, R.G. Astaxanthin: Sources, extraction, stability, biological activities and its commercial applications—A review. *Mar. Drugs* 2014, *12*, 128-152.

[29] Pashkow, F.J.; Watumull, D.G.; Campbell, C.L. Astaxanthin: A novel potential treatment for oxidative stress and inflammation in cardiovascular disease. *Am. J. Cardiol.* 2008, *101*, 58D–68D.

[30] Roche, F. Astaxanthin: Human food safety summary. In Astaxanthin As a Pigmenter in Salmon Feed, Color Additive Petition 7C02 1 1, United States Food and Drug Administration; Hoffman-La Roche Ltd.: Basel, Switzerland, 1987; p. 43.

[31] Augusti, P.R.; Quatrin, A.; Somacal, S.; et al. Astaxanthin prevents changes in the acticities of thioredoxin reductase and paraoxonase in hypercholesterolemic rabbits. *J. Clin. Biochem. Nutr.* 2012, *51*, 42-49.

[32] Kamath,B.S.; Srikanta, B.M.; Dharmesh, S.M.; et al. Ulcer preventive and antioxidative properities of astaxanthin from *Haematococcus pluvialis*. *Eur. J. Pharmacol*. 2008, *590*, 387-395.

[33] Ranga, R.A.; Sindhuja, H.N.; Dharmesh, S.M.; et al. Effetive inhibition of skin cancer, tyrosinase and antioxidantive properties by astaxanthin and astaxanthin esters from the green alga *Haematococcus pluvialis*. *J. Agric. Food Chem.* 2013, *61*, 3842-2851.

[34] Goto, S.; Kogure, K.; Abe, K.; et al. Efficient radical trapping at the surface and inside the phospholipid membrane is responsible for highly potent antiperoxidative activity of the carotenoid astaxanthin. *Biochim. Biophys. Acta.* 2011, *1512*, 251-258.

[35] Ranga, R.A.; Baskaran, V.; Sarada, R.; et al. In vivo bioavailability and antioxidant activity of carotenoids from micoalgal biomass-A repeated dose study. *Food Res. Int.* 2013, *54*, 711-717.

[36] Ranga, R.A.; Raghunath, R.R.L, Baskaran, V.; et al. Characterization of microalgal carotenoids by mass spectrometry and their bioavailability and antioxidant properties elucidated in rat model. *J. Agric. Food Chem.* 2010, *58*, 8553-8559.

[37] Ranga, R.A.; Sarada, R.; Baskaran, V.; et al. Identification of carotenoids from green alga *Haematococcus pluvialis* by HPLC and LC-MS (APCI) and their antioxidant properties. *J. Microbiol. Biotechnol.* 2009, *19*, 1333-1341.

[38] Bennedsen, M.; Wang, X.; Willen, R.; et al. Treatment of *H.pylori i*nfected mic with antioxidant astaxanthin reduced gastric inflammation, bacterial load and modulates cytokine release by splenocytes. *Immunol. Lett.* 1999, *70*, 185-189.

[39] Park, J.S.; Chyum, J.H.; Kim, Y.K.; et al. Astaxanthin decreased oxidative stress and in flammation and enhanced immune response in humans. *Nutr. Metab.* 2010, *7*, 1-10.

[40] Uchiyama, K.; Naito, Y.; Hasegawa, G.; et al. Astaxanthin protects β-cells against glucose toxicity in diabetic db/db mice. *Redox. Rep.* 2002, *7*, 290-293.

[41] Otton, R.; Marin, D.P.; Bolin, A.P.; et al. Astaxanthin ameliorates the redox imbalance in lymphocytes of experimental diabetic rats. *Chem. Biol. Interact.* 2010, *186*, 306-315.

[42] Jyonouchi, H.; Sun, S.; Iijima, K.; et al. Antitumor activity of astaxanthin and its mode of action. *Nutr. Cancer* 2000, *36*, 59-65.

[43] Nakao, R.; Nelson, O.L.; Park, J.S.; et al. Effect of dietary astaxanthin at different stages of mammary tumor in BALB/c mice. *Anticancer Res.* 2010, *30*, 2171-2175.

[44] Fassett, R.G.; Combes, J.S. Astaxanthin: A potential therapeutic agent in cardiovascular disease. *Mar. Drugs* 2011, *9*, 447-465.

[45] Monroy-Ruiz, J.; Sevilla, M.A.; Carrón, R. Astaxanthin-enriched-diet reduces blood pressure and improves cardiovascular parameters in spontaneously hypertensive rats. *Pharmacol. Res.* 2011, *63*, 44-50.

[46] Nakao, R.; Nelson, O.L.; Park, J.S. et al. Effect of astaxanthin supplementation on inflammation and cardiac function in BALB/c mice. *Anticancer Res*. 2010, *30*, 2721-2725.

[47] Park, J.S.; Mathieson, B.D.; Hayek, M.G. et al. Astaxanthin stimulates cell-mediated and humoral immune responses in cats. *Vet. Immune Immunopathol.* 2011, *144*, 455-461.

[48] Manabe, E.; Handa, O.; Naito, Y.; Mizushima, K.; Akagiri, S.; Adachi, S.; Takagi, T.; Kokura, S.; Maoka, T.; Yoshikawa, T. Astaxanthin Protects Mesangial Cells from Hyperglycemia-Induced Oxidative Signaling. *J. Cell. Biochem.* 2008, *103*, 1925-1937.

[49] Wolf, A.M.; Asoh, S.; Hiranuma, H.; Ohsawa, I.; Iio, K.; Satou, A.; Ishikura, M.; Ohta, S. Astaxanthin Protects Mitochondrial Redox State and Functional Integrity Against Oxidative Stress. *J. Nutr. Biochem.* 2010, *21*, 381-389.

[50] Zhang, Z.W.; Xu, X.C.; Liu, T.; Yuan, S. Mitochondrion-Permeable Antioxidants to Treat ROS-Burst-Mediated Acute Diseases. *Oxid. Med. Cell Longev.* 2016, *1*, 6859523.

[51] Kuroki, T.; Ikeda, S.; Okada, T.; Maoka, T.; Kitamura, A.; Sugimoto, M.; Kume, S. Astaxanthin Ameliorates Heat Stress-Induced Impairment of Blastocyst Development in Vitro: Astaxanthin Colocalization with and Action on Mitochondria. *J. Assist. Reprod. Genet.* 2013, *30*, 623-631.

[52] Song, X.D.; Wang, B.S.; Lin, S.C.; Jing, L.L.; Mao, C.P.; Xu, P.; Lv, C.J.; Liu, W.; Zuo, J. Astaxanthin Inhibits Apoptosis in Alveolar Epithelial Cells Type II in Vivo and in Vitro Through the ROS-dependent Mitochondrial Signalling Pathway. *J. Cell. Mol. Med.* 2014, *18*, 2198–2212.

Chapter II

The effect of AX on muscle atrophy induced by mitochondrial oxidative stress and dysfunction

2.1 Introduction

Skeletal muscle atrophy has been observed in muscle disuse during unloading, immobilization, denervation, fasting, aging, and several disease conditions. Unloading-related muscle loss caused by prolonged bed rest or spaceflight specifically occurs in antigravity muscles including in slow muscle fibers [1,2]. It has been known that the number of mitochondria in slow muscle fibers is higher than that in fast muscle fibers [3]. Mitochondria are the main energy source of skeletal muscles that produce adenosine triphosphate (ATP) through OXPHOS. In this process, 0.2-2.0% of diatomic oxygen passes through the electron transport chain complexes I and III and incompletely reduces leaked electrons to superoxide anions [4]. Mitochondria play a vital role in disused skeletal muscle atrophy [5] and mitochondrial signaling can contribute to disuse muscle atrophy in three major ways [6-8]: (1) increased mitochondrial reactive oxygen species (ROS) production, (2) energy stress: decrease in ATP production and the activation of AMPK, (3) mitochondria release of pro-apoptotic factors: release of cytochrome c into the cytosol and active caspase 3. In fact, the increase of mitochondrial ROS production could participate in both the energy stress and apoptosis [9]. Therefore, mitochondrial ROS has major impact on disuse-related muscle atrophy, and the development of antioxidants to prevent the increase in mitochondrial ROS in muscle due to inactivity has been extensively researched.

Although antioxidants have been shown to prevent muscle atrophy [17,18], their mechanisms of action vary owing to their different characteristics. Some studies have shown that AX might have an effect on muscle atrophy [19,20]; however, its mechanism of action in mitochondria remains unclear. This part investigated the effect of AX on muscle atrophy

induced by mitochondrial oxidative stress and dysfunction. Sol8 cells (slow-type muscle cells extracted from the soleus muscle) were used to explore the underlying mechanisms.

2.2 Materials and methods

2.2.1 Animal model

Male C57BL/6J mice (Japan CLEA, Tokyo, Japan) (6 weeks old) were housed in a room maintained at 24 ± 1 °C and a 12 h light/dark cycle with food (Oriental Yeast Company, Tokyo, Japan) and water available ad libitum. After 1 week of acclimatation, mice were randomized into four groups: control mice fed the normal diet (C-ND, n = 6); tail-suspension mice fed the normal diet (S-ND, n = 6); control mice fed the AX diet (C-AX, n = 6); and tail-suspension mice fed the AX diet (S-AX, n = 6). An AX-supplemented diet (0.2%, w/w) or a normal diet was fed to mice for four weeks. Since then, these mice (11 weeks old) were subjected to tail suspension to establish the muscle atrophy model. Briefly, the mouse tail was fixed with medical tape; the other end of the tape was attached to the top of the cage to keep its body at a 30 degree angle with the surface (Photo 2-1). The forelimbs were free to move on the ground to enable free access to water. During the development of tail suspension-induced muscle atrophy, the mice continued to receive normal or AX-supplemented diets until termination of the experiment two weeks later. The soybean oil content of the AX-supplemented diet was reduced to adjust for the composition of other nutrients. The AX-supplemented diet comprised the normal diet (based on AIN-93G) mixed with BioAstin SCE (containing 10.84% AX; Toyo Koso Kagaku Co. Ltd., Chiba, Japan). The nutritional composition of each diet is shown in Table 2-1, the right hindlimb skeletal muscles including the tibialis anterior (TA), extensor

digitorum longus (EDL), gastrocnemius (GA), and soleus (SO) muscles were isolated at the time of sacrifice. After measuring the wet weight, the skeletal muscles were immediately frozen in chilled isopentane with liquid nitrogen and stored at -80 ˚C until analysis. All animal experiments were approved by the Committee on Animal Experiments of Nagasaki University (permission no. 1803291443) and performed according to the guidelines for the care and use of laboratory animals set by the University.

Photo 2-1. Tail-suspension model (Normal diet and AX diet)

Normal diet_
tail-suspension

AX diet_
tail-suspension

Table 2-1. Nutritional composition of normal diet and AX diet

	Normal	AX
α-corn starch (g)	45.4	45.4
Sucrose (g)	22.8	22.8
Casein (g)	20	20
Cystine (g)	0.3	0.3
Soybean oil (g)	5	4.8
Bio Astin SCE (g)	0	0.2
Vitamin mix (g)	1	1
Mineral mix including choline (g)	3.5	3.5
Cellulose (g)	2	2
Tertiary butylhydroquinone (g)	0.0014	0.0014

(Bio Astin SCE: oleoresin extracted from Haematococcus pluvialis, containing 10.84% AX)

2.2.2 Multicolor immunofluorescence staining

The separated SO muscle was placed on the gum tragacanth and immediately frozen in chilled isopentane with liquid nitrogen and stored at -80 °C until analysis. The mid-belly transverse cryosections of SO muscles (5 μm thickness) were made with LEICA CM1950 cryostat (Wetzlar, Germany). Sections were put on poly-L-lysine-coated slide glasses, fixed in ice-cold acetone, and stained using multicolor immunofluorescence antibodies as described previously [21]. Primary antibody reactions were performed using anti- myosin heavy chain (MHC) type I (BA-F8), anti-MHC IIa (SC-71), and anti-MHC IIb (BF-F3) (DSHB, Iowa City, IA, USA); the secondary antibodies used were anti-mouse Alexa Fluor 350 IgG_{2b}, anti-mouse Alexa Fluor 488 IgG_1, and anti-mouse Alexa Fluor 555 IgM, respectively (Thermo Fisher

Scientific, Waltham, MA, USA). Images were acquired using a BIOREVO BZ-X710 microscope (Keyence, Osaka, Japan).

2.2.3 Measurement of muscle fiber cross-sectional area (CSA)

For fiber type analysis, all fibers within the entire cross-section were characterized. At least 600 myofiber cross-sectional areas (CSAs) were measured per group.

2.2.4 Cell culture

Sol8 myoblastic cells were obtained from the American Type Culture Collection (Rockville, MD, USA). They were seeded in a collagen-coated plate and cultured in Dulbecco's modified Eagle medium (DMEM) supplemented with 10% fetal bovine serum (FBS), 100 units/mL penicillin, and 100 μg/mL streptomycin and maintained at 37 °C in a 5% CO_2 environment. At a confluence of 100%, sol8 myoblasts were fused by shifting the medium to DMEM supplemented with 2% horse serum (HS). Cells were maintained in 2% HS/DMEM (differentiation medium) for 4 days for the formation of myotubes, as described previously.

2.2.5 Isolation of mitochondria

Mitochondria from Sol8 cells, and skeletal muscle from C57BL/6J mice were prepared as previously [23,24]. Briefly, tissues or cells were minced in ice-cold CP-1 buffer (100 mM KCl, 50 mM Tris-HCl, 2 mM EGTA, pH 7.4). After homogenization by a plastic electric rod, then centrifuged at 500 ×*g* for 10 min. The supernatant was collected and further centrifuged for 10 min at 10,500 ×*g* to obtain the mitochondrial pellet and cytosolic fraction.

2.2.6 Detection of AX in mitochondrial and cytosolic fractions

The AX contents in mitochondrial and cytosolic fractions from Sol8 myotubes were prepared, as described previously [23]. Briefly, Sol8 myotubes were treated with AX (100 nmol) or DMSO, as control, in 10 mL culture medium/100 mm dishes and incubated at 37 °C with 5% CO_2 for 24 h. The cells were harvested to isolate the mitochondrial fraction as described in Section 2.2.5. After lyophilization, crude mitochondrial extracts and cytosol were solubilized in acetone and centrifuged at 12,000 ×*g* for 15 min. The supernatants were filtered using a 0.45 μm polytetrafluorethylene membrane and analyzed using HPLC and a spectrophotometer detector (JASCO, Tokyo, Japan) set at 460 nm. A Shim-pack CLC-ODS column (150 mm length and 6.0 mm internal diameter) was used.

2.2.7 Detection of H_2O_2 production

The rate of H_2O_2 production by isolated mitochondria was detected using a fluorescent probe, Amplex Red, as described previously [24]. Mitochondria from muscle tissues were suspended in a buffer containing 5 mM 3-(N-morpholino) propanesulfonic acid (MOPS) (pH 7.4), 70 mM sucrose, and 220 mM mannitol, and mitochondria protein concentration was determined by using a bicinchoninic acid (BCA) protein assay (Pierce, Rockford, IL, USA). Mitochondria (30 μg mitochondrial protein per well) were incubated in black 96-well plates with a reaction mixture containing 50 μM Amplex Red, 2 U/mL horseradish peroxidase, 30 U/mL superoxide dismutase (SOD), 10 mM succinate, 10 μM antimycin A as substrate at room temperature for 30 min, protected light. SOD was added to convert all superoxide into H_2O_2.

SOD was added to convert all superoxide into H_2O_2. The rate of H_2O_2 production was linear with respect to mg of mitochondrial protein.

2.2.8 Measurement of mitochondrial superoxide levels

Dihydroethidium (DHE) was used as a second method for the detection of superoxide. Differentiated Sol8 myotubes were plated in 96-well black plates (3×10^3 cells/well) and treated with DMSO or AX for 24 h. After washing with HBSS, the cells were then incubated with HBSS containing 10 mM succinate, 10 μM antimycin A, and 5 μM DHE for 30 min. Fluorescence was recorded using a microplate reader (BioTek Cytation 3, Winooski, VT, USA) at excitation and emission wavelengths of 490 and 595 nm, respectively [24].

2.2.9 Measurement of mitochondrial membrane potential

MMP was detected using the fluorescent probe, JC-1 dye (Thermo Fisher Scientific). Differentiated Sol8 myotubes were plated in 96-well black plates and pretreated with DMSO or AX for 1 h, followed by the addition of 25 μM antimycin A for 48 h. After washing with PBS, the cells were incubated with 1.5 μM JC-1 dye at 37 °C for 30 min. MMP was quantified using a microplate reader (BioTek Cytation 3) at 550 nm excitation/600 nm emission and 485 nm excitation/535 nm emission wavelengths. The quantitative MMP value was expressed as the relative ratio of aggregate-to-monomer values of fluorescence intensity. Carbonyl cyanide m-chlorophenyl hydrazone (CCCP) was used as a negative control to normalize changes in the membrane.

2.2.10 Quantitative real-time polymerase chain reaction (qRT-PCR)

Total RNA was extracted from muscle using an acid guanidinium thiocyanate-phenol-chloroform mixture (ISOGEN; Nippon Gene, Tokyo, Japan). Real-time RT-PCR was performed with the appropriate primers and SYBR Green dye using a real-time PCR system (ABI Real-Time PCR Detection System; Applied Biosystems, Foster City, CA, USA), as described previously [25]. The oligonucleotide primers used for PCR are shown in Table 2-2.

2.2.11 Immunoblotting

Mouse SO muscles and Sol8 were prepared in lysis buffer containing 50 mM Tris-HCl, pH 7.5, 150 mM NaCl, 1% Triton X-100, 5 mM EDTA, 10 mM NaF, 2 mM Na_3VO_4, and a protease inhibitor cocktail tablet without EDTA (Roche Diagnostics, Indianapolis, IN, USA), and homogenized using a sonicator. The cytosolic fraction for the analysis of cytochrome c release was prepared as described in Section 2.2.5. The Pierce BCA assay (Pierce, Rochford, IL, USA) was used to quantify proteins. Protein samples were combined with 4× sample buffer (250 mM Tris-HCl, 8% SDS, 40% glycerol, 8% beta-mercaptoethanol, and 0.02% bromophenol blue) and subjected to SDS-PAGE. The proteins were transferred onto a polyvinylidene difluoride (PVDF) membrane and probed with primary antibodies according to the manufacturer's instructions. Anti-β-actin (Gene Tex, AC-15, Irvine, CA, USA), anti-cleaved caspase 3 (Cell Signaling Technology, #9661, Danvers, MA, USA), anti-caspase 3 (Cell Signaling Technology, #9662, Danvers, MA, USA), anti-cytochrome c (Santa Cruz Biotechnology, sc-13156, Santa Cruz, CA, USA), anti-glyceraldehyde 3-phosphate dehydrogenase (GAPDH) (Santa Cruz Biotechnology, sc-25778), anti-total OXPHOS (Abcam,

Table 2-2. The oligonucleotide primers and sequence

Target gene		Sequence
AMPK alpha-1	F	5'- TCAGTTCCTGGAGAAAGATGG-3'
	R	5'- TTATGTCCGGTCAACTCGTG-3'
PPAR gamma	F	5'- CCCATCGAGGACATCCAA-3'
	R	5'- CACGTGCTCTGTGACGATCT-3'
Ckmt 2	F	5'- TACTCACGGGCAGTTTGATA-3'
	R	5'- CACATTCTCCACCTCCCTTC-3'
Ucp2 f	F	5'- GCGTTCTGGGTACCATCCTA-3'
	R	5'- AGAGTCGTAGAGGCCAATGC-3'
Atp5g1	F	5'- CCATCTAAGCAGCCTTCCTG-3'
	R	5'- GATCCAGCCACACCAACTGT-3'
Ndufaf2	F	5'- AGGCATGAGCTGGTGGTC-3'
	R	5'- TCTGCCCTCTCCAGTTCTTG-3'
Sdhb	F	5'- GGAGGGCAAGCAACAGTATC-3'
	R	5'- CTTGTCTCCGTTCCACCAGT-3'
Gapdh	F	5'- ACCCAGAAGACTGTGGATGG -3'
	R	5'- TTCAGCTCTGGGATGACCTT - 3'

F, forward primer; R, reversed primer; *AMPK*, Adenosine 5'-monophosphate (AMP)-activated protein kinase; *PPAR*, peroxisome proliferator-activated receptor; *Ckmt*, creatine kinase in mitochondria; *Ucp*, uncoupling protein; *Atp5g1*, ATP synthase, H^+ transporting, mitochondrial F0 complex, subunit C1; *Ndufaf2*, NADH-ubiquinone oxidoreductase complex assembly factor; *Sdhb*, succinate dehydrogenase complex, subunit B; *Gapdh*, glycelaldehyde-3-phosphate dehydrogenase.

ab110413, Cambridge, UK), and anti-VDAC1/Porin (Abcam, ab14734, Cambridge, UK) were used. Donkey anti-rabbit IgG at 1:5000 (GE Healthcare, Little Chalfont, UK) and sheep anti-mouse IgG at 1:5000 (GE Healthcare, Little Chalfont, UK) were used as the secondary antibodies. Membranes were developed using ImmunoStar® Zeta Western blotting detection reagents (Fujifilm Wako Pure Chemical Corporation, Osaka, Japan). Immunocomplexes on the membrane were analyzed by Image J software (National Institutes of Health, Bethesda, MD, USA).

2.2.12 Statistical analysis

All data were analyzed by one-way/two-way analysis of variance (ANOVA), using SPSS statistics software, followed by the Tukey test for individual differences between groups. *p*-values <0.05 were considered to indicate significant differences.

2.3 Results

2.3.1 Effect of dietary AX on food intake and body weight in tail-suspension mice

From food intake data, we found that 0.55 ± 0.15 mg/day of AX was fed to each mouse. There was no significant difference between the normal and AX-supplemented diet groups in food intake (Figure 2-1A). Although the body weights of mice in the S-ND and S-AX groups significantly decreased after tail-suspension, these differences were not significant (Figure 2-1B).

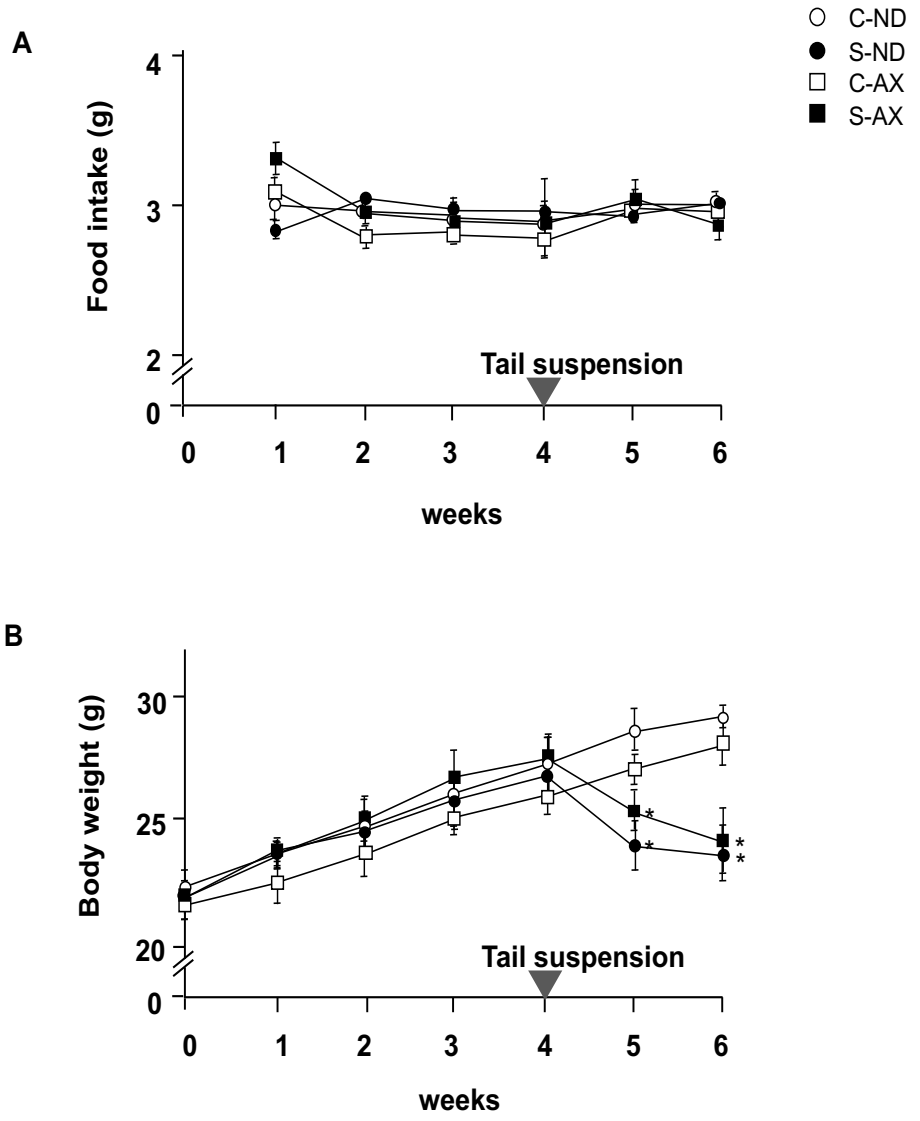

Figure 2-1. Changes in food intake and body weight with the AX diet: (A) food intake; (B) body weight. Mice were fed an AX or normal diet for 6 weeks. They were subjected to tail suspension since week 4, which continued for 2 weeks (C-ND, $n = 6$; S-ND, $n = 6$; C-AX, $n = 6$; S-AX, $n = 6$). Data are presented as mean ± S.D. ($n = 6$). Statistical analysis was performed by the two-way ANOVA and Tukey test. * $p < 0.05$, compared with ND. C-ND, control mice fed the normal diet; S-ND, tail-suspension mice fed the normal diet; C-AX, control mice fed the AX diet; and S-AX, tail suspension mice fed the AX diet. Arrow means the time of tail suspension.

2.3.2 Effect of dietary AX on muscle mass and fiber size in tail-suspension mice

To examine the effect of AX on weight gain in mice, we compared the wet weights of several muscles in the normal control and tail-suspension mice fed a normal or AX-supplemented diet.

Tail suspension significantly decreased the weights of TA, GA, and SO muscles, but not that of the EDL (Figure 2-2). In comparison to the S-ND group, the S-AX group showed inhibition of muscle-weight reduction only in the SO. In contrast, AX supplementation failed to prevent tail suspension-induced muscle atrophy in the EDL, TA, and GA muscles.

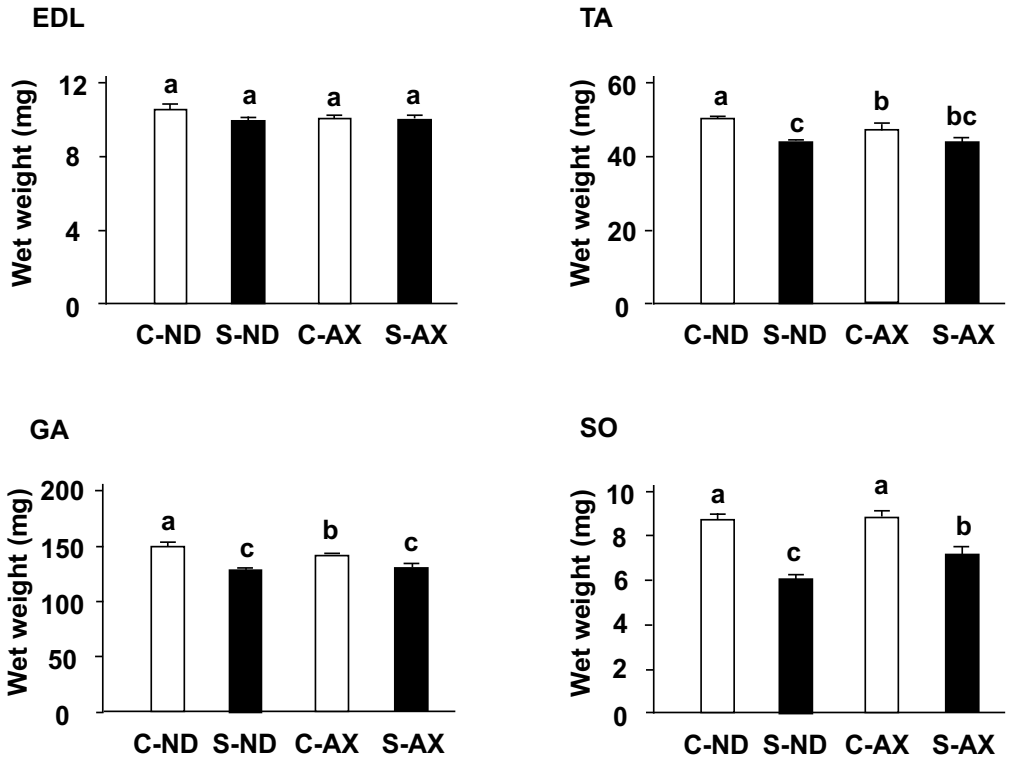

Figure 2-2. The effect of dietary AX on muscle mass in tail-suspension mice. The wet weights of the tibialis anterior, extensor digitorum longus, gastrocnemius, and soleus muscles were measured. Data are presented as mean ± S.D. (n = 6). Different letters indicate significant differences ($p < 0.05$) based on the two-way ANOVA and Tukey's test. C-ND, control mice fed the normal diet; S-ND, tail-suspension mice fed the normal diet; C-AX, control mice fed the AX diet; and S-AX, tail-suspension mice fed the AX diet. TA, tibialis anterior muscle; EDL, extensor digitorum longus muscle; GA, gastrocnemius muscle, SO, soleus muscles.

Next, we analyzed the cross-sectional area (CSA) of the SO muscle fiber. It has been reported that tail-suspension affects slow fiber type muscles, especially type I and IIa, but not fast fiber type ones [26]. Because the soleus muscle is made up of type I fiber (30.6% ± 2.2%), type IIa fiber (49.1% ± 1.2%), type IIx (11.8% ± 1.7%), and other types of fibers, we performed different fiber typing to investigate which type of fiber was influenced by AX [21]. Multicolor immunofluorescent staining showed that it comprised MHC type I (blue) and IIa (green) myofibers. Type IIb (red) myofibers were hardly detected in the SO muscle fibers. Myofibers in the S-ND group showed decreased CSA staining and comprised type I and IIa fibers (Figure 2-3A), compared to the C-ND group. In contrast, the CSAs of muscle fibers stained with type I and IIa in the S-AX mice were similar to those observed in the C-AX mice (Figure 2-3A). We confirmed the average CSA of types I and IIa fibers in the SO muscle. Consistent with the results that indicated a decrease in muscle weights in the S-ND group, the average CSA of type I and IIa muscle fibers in the S-ND group was significantly decreased, compared to that in the C-ND group. Meanwhile, AX prevented the decrease of CSA caused by tail suspension and resulted in the increase of CSA rather than the reduction of CSA (Figure 2-3B). In particular, tail suspension in the S-AX group showed inhibition of the CSA reduction of muscle fibers of MHC type I and IIa.

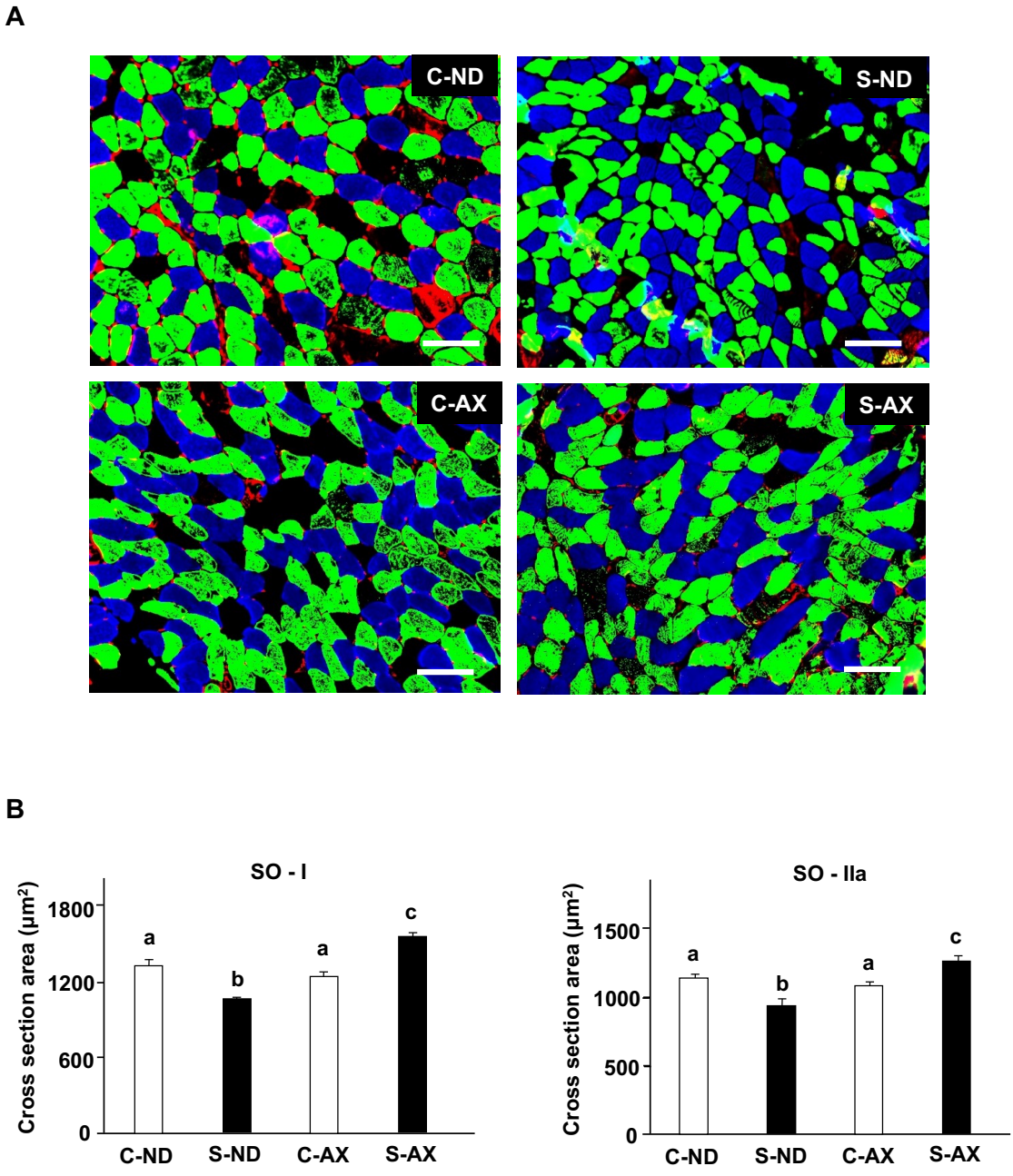

Figure 2-3. Effect of dietary AX on cross-sectional area (CSA) and fiber size in the soleus (SO) muscle of tail-suspension mice. (A) Sections (5 μm thickness) of SO muscle from C-ND, S-ND, C-AX, and S-AX groups, with multicolor immunofluorescence staining. Scale bar = 100 μm. Magnification, ×20; (B) The average CSA of type I and type IIa fibers in the SO muscle. Data are presented as mean ± S.D. (n = 3). Different letters indicate significant differences (p < 0.05) based on the one-way ANOVA and Tukey's test. C-ND, control mice fed the normal diet; S-ND, tail-suspension mice fed the normal diet; C-AX, control mice fed the AX-supplemented diet; and S-AX, tail-suspension mice fed the AX-supplemented diet.

2.3.3 Effect of dietary AX on H_2O_2 production in the muscle of tail-suspension mice

Excessive ROS including superoxide anions produced by mitochondria play a vital role in disused skeletal muscle atrophy [5,6]. In the measurement of H_2O_2 production by using Amplex Red, all superoxide ions have been converted into H_2O_2 by SOD. The amount of H_2O_2 production was significantly increased by tail suspension in normal diet mice (S-ND group). In contrast, the AX-supplemented diet inhibited the increase of H_2O_2 production in the S-AX group (Figure 2-4).

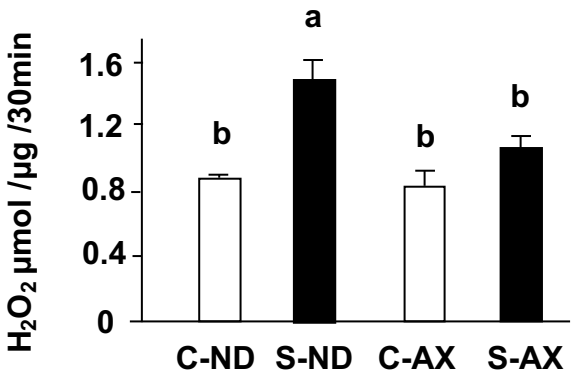

Figure 2-4. Effect of dietary AX on H_2O_2 production in the muscle of tail-suspension mice. The rate of H_2O_2 production from isolated mitochondria in muscle was detected by Amplex Red fluorescence. Data are represented as mean ± S.D. (n = 6). Different letters indicate significant differences ($p < 0.05$) based on the one-way ANOVA and Tukey's test. C-ND, control mice fed the normal diet; S-ND, tail-suspension mice fed the normal diet; C-AX, control mice fed the AX-supplemented diet; and S-AX, tail-suspension mice fed the AX-supplemented diet. H_2O_2 production are representative of at least three independent studies.

2.3.4 Effect of dietary AX on oxidative phosphorylation respiration in the muscle of tail-suspension mice

Denervation-induced muscle atrophy reportedly impairs oxidative phosphorylation complex proteins in mitochondria [27]. In addition, we found AX prevented the increase of H_2O_2 production caused by tail suspension. Thus, we investigated the effect of AX on the levels of oxidative phosphorylation-related protein complexes in the muscle. The amounts of complexes I and III in the SO muscle of the S-ND group were significantly lower than that of the C-ND group. In contrast, there were no significant changes between the protein complexes in the C-AX and S-AX groups (Figure 2-5).

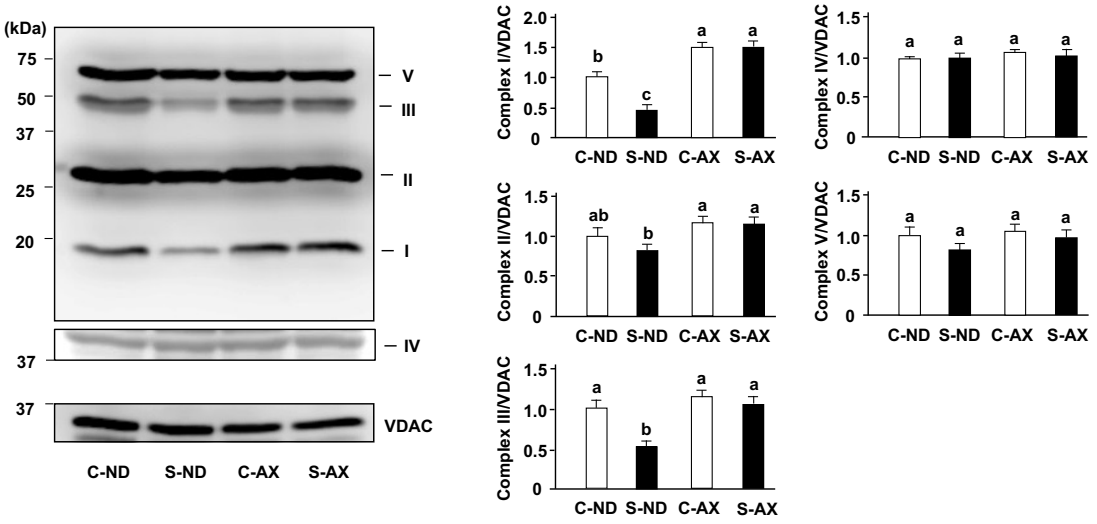

Figure 2-5. Effect of dietary AX on the expression of oxidative phosphorylation (OXPHOS)-related protein complexes in SO muscle of tail-suspension mice. Proteins (20 μg/lane) were extracted from the SO muscle and subjected to SDS-PAGE and transferred onto a PVDF membrane. Immunoblotting for total OXPHOS was performed. Data are represented as mean ± S.D. ($n = 6$). Different letters indicate significant differences ($p < 0.05$) based on the one-way ANOVA and Tukey's test. C-ND, control mice fed the normal diet; S-ND, tail-suspension mice fed the normal diet; C-AX, control mice fed the AX-supplemented diet; and S-AX, tail-suspension mice fed the AX-supplemented diet. Immunoblotting experiments are representative of at least three independent studies.

2.3.5 Effect of dietary AX on mitochondrial biogenesis in the muscle of tail-suspension mice

When muscles undergo immobilization and denervation, a series of undesirable changes occur in the mitochondria of the muscle, including inhibition of mitochondrial biogenesis [28]. Moreover, it has been reported that AX treatment stimulates mitochondrial biogenesis in the skeletal muscle [29]. Consistent with previous reports, we found that *AMPKα-1* and *PPAR-γ* mRNA expressions in the S-ND group were significantly decreased, compared with those in the C-ND group, whereas the S-AX group showed inhibition of the decrease of these mRNA expressions in SO muscle. In addition, the expression of *Ckmt2* mRNA in the S-AX group was significantly higher than that in the S-ND group. Although there were no significant differences between S-ND and S-AX in the expression of *Ucp2*, *Atp5g1, and Sdhb*, AX slightly improved the expression in tail-suspension mice (Figure 2-6).

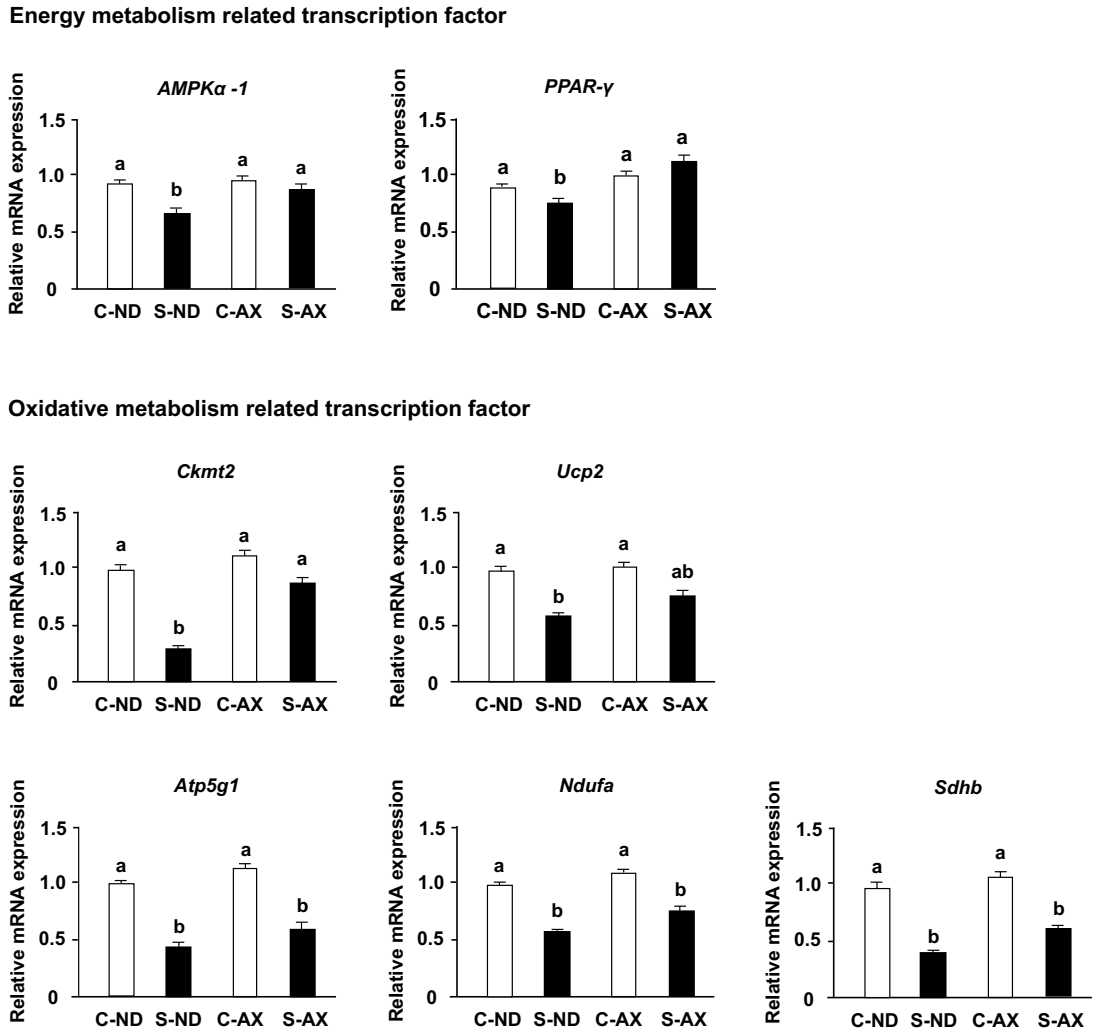

Figure 2-6. Effect of dietary AX on mitochondrial biogenesis in SO muscle of tail-suspension mice. The total RNA of the SO muscle was extracted and subjected to real-time PCR. Expression ratio relative to that of *glycelaldehyde-3-phosphate dehydrogenase (GAPDH)*. Data are represented as mean ± S.D. (n = 6). Different letters indicate significant differences (p < 0.05) based on the one-way ANOVA and Tukey's test. Real-time PCR experiments are representative of at least three independent studies. *AMPK,* adenosine 5'-monophosphate (AMP)-activated protein kinase; *PPAR,* peroxisome proliferator-activated receptor; *Ckmt,* creatine kinase in mitochondria; *UCP,* uncoupling protein; *Atp5g1,* ATP synthase, H+ transporting, mitochondrial F0 complex, subunit C1; *Ndufaf2,* NADH-ubiquinone oxidoreductase complex assembly factor; *Sdhb,* succinate dehydrogenase complex, subunit B.

2.3.6 Location of AX in Sol8 myotubes

Manabe et al. reported that AX is more likely to accumulate in the mitochondria of mesangial cells [30]. This finding and the results of our *in vivo* experiments implied that AX may target the mitochondria. To investigate the effect of AX on mitochondrial function, we determined the location of AX in the mitochondria by using Sol8 myotubes derived from SO. Although differentiated Sol8 myotubes contained myoblasts, myotubes' differentiation marker (slow type myosin heavy chain) was detected in Sol8 myotubes (data not shown). Therefore, these cells were used in subsequent experiments. We found that AX was preferentially detected in the mitochondrial fraction, which was approximately 1% that of the AX treatment concentration in Sol8 myotubes; DMSO (0 nmol AX) was detected neither in the mitochondria nor in the cytosol (Table 2-3). This result was consistent with a previous report that AX is more likely to accumulate in the mitochondria in mesangial cells [30].

Table 2-3. AX content in mitochondria and cytosol of AX-treated Sol8 myotubes.

AX treatment	AX content (nmol)	
	Cytosol	Mitochondria
0 nmol	N.D	N.D.
100 nmol	0.09 ± 0.01	1.07 ± 0.02

Data are presented as mean ± S.D. (n = 3). N.D.: not detected.

2.3.7 Effect of AX on mitochondrial function in Sol8 myotubes

Next, we analyzed the effect of AX on mitochondrial ROS generation and MMP levels in Sol8 myotubes treated with antimycin A (AnA), a complex III inhibitor. Mitochondrial ROS production in AnA-treated Sol8 myotubes was significantly increased compared to that in non-treated cells. The increased production of complex III-driven ROS was significantly suppressed by AX treatment in a dose-dependent manner (Figure 2-7A). Addition of AX in AnA non-treated Sol8 myotubes did not influence MMP (Figure 2-7B). AnA treatment significantly decreased the MMP in Sol8 myotubes relative to non-treated cells, resulting in the same MMP level as that of the negative control, with the uncoupler CCCP. Nevertheless, improvements in MMP levels were noticed in the AX-treated cells, although there were no significant differences between the different AX concentrations. These results suggested that AX pretreatment may inhibit mitochondrial ROS production and maintain the MMP in Sol8 myotubes. These results indicated that AX has a role in mitochondrial protection.

A

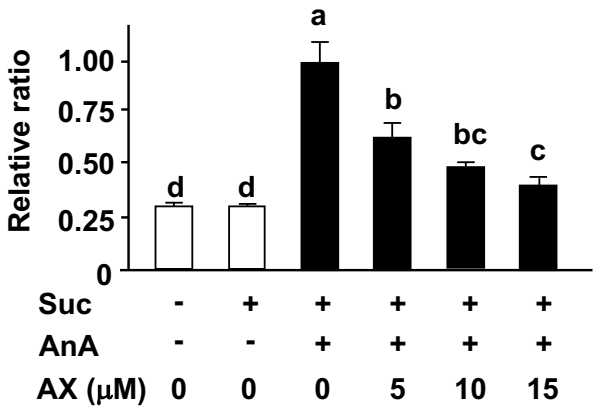

B

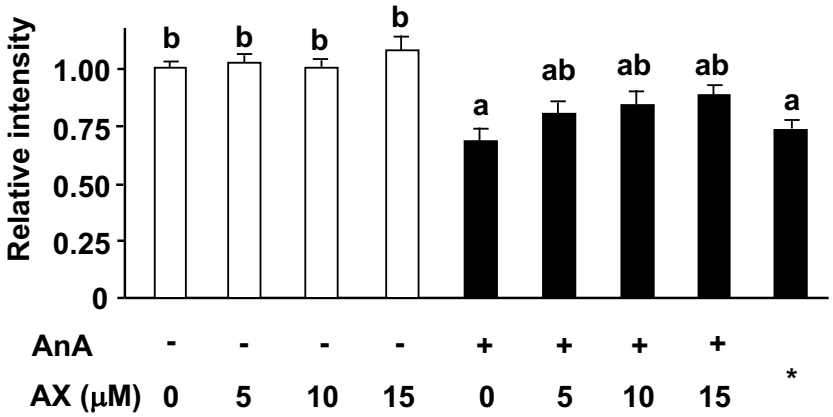

Figure 2-7. Effect of AX on mitochondrial superoxide levels and MMP in AnA-treated Sol8 myotubes: (A) The rate of superoxide formation in AX-treated Sol8 myotubes was assessed using dihydroethidium (DHE) fluorescence. Succinate and AnA were used as respiratory complex II substrate and complex III inhibitor, respectively; (B) The quantitative mitochondrial membrane potential (MMP) values were calculated based on the ratio of fluorescence intensity values (JC-1 dye). Data are represented as mean ± S.D. (n = 8). Different letters indicate significant differences ($p < 0.05$) based on the one-way ANOVA and Tukey's test. "-" represents DMSO; *, CCCP; Suc, succinate; AnA, antimycin A. ROS production and MMP levels experiments are representative of at least three independent studies.

2.3.8 Effect of AX on the expression of apoptosis-related proteins in AnA-treated Sol8 myotubes

To explore the mitochondria-mediated apoptotic mechanism of AX in AnA-treated Sol8 myotubes, the release of cytochrome c into the cytosol (Figure 2-8A) and activation of caspase 3 (Figure 2-8B) were examined. The amount of cytochrome c in AnA-treated Sol8 myotubes, without AX, in the cytosolic fraction was significantly increased compared to that of the DMSO-treated control group (Figure 2-8A). In contrast, AX inhibited the release of cytochrome c into the cytosol of AnA-treated Sol8 myotubes. Furthermore, AnA treatment tended to increase the amount of cleaved caspase 3 in Sol8 myotubes, whereas AX effectively decreased the amount of cleaved caspase 3 in AnA-treated Sol8 myotubes (Figure 2-8B).

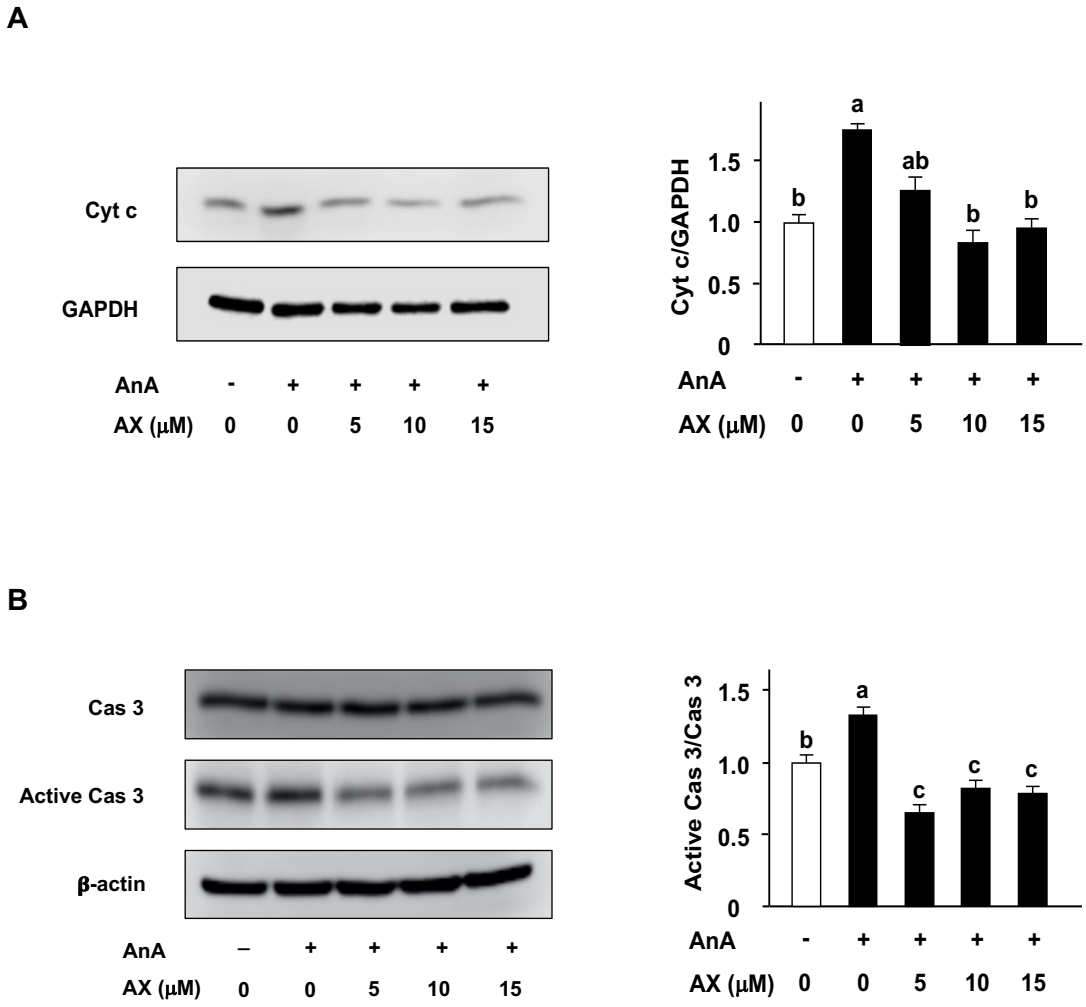

Figure 2-8. Effect of AX on the activation of apoptosis-related proteins in AnA-treated Sol8 myotubes: (A) Sol8 myotubes were treated with different AX concentrations for 1 h, then AnA (25 μM) was added for 48 h. The cytosolic fraction was subjected to SDS-PAGE and transferred onto a PVDF membrane. Immunoblotting for cyt c and GAPDH was performed on different membranes without antibody stripping, as described in Section 2.6. The ratio of cyt c proteins to GAPDH was calculated using densitometric analysis; (B) Sol8 myotubes were treated with different AX concentrations for 1 h and with AnA (25 μM) for 48 h before total proteins were extracted. Proteins (20 μg/lane) were extracted from Sol8 myotubes and subjected to SDS-PAGE, then transferred onto a PVDF membrane. Immunoblotting for cyt c, cas 3, and active cas 3 was performed on different membranes without antibody stripping, as described in Section 2.6. Data are presented as mean ± S.D. (n = 3). Different letters indicate significant differences ($p < 0.05$) based on the one-way ANOVA and Tukey's test. AnA, antimycin A; cyt c, cytochrome c; and cas 3, caspase 3. Immunoblotting experiments are representative of at least three independent studies.

2.4 Discussion

The novel findings of this research revealed that dietary AX supplementation attenuated the decrease in muscle mass and myofibers in the SO muscle, preventing mitochondrial dysfunction caused by oxidative stress. AX particularly inhibited the reduction of mitochondrial complexes I and III protein content and regulated mitochondrial oxidative phosphorylation and biogenesis in the SO muscle of tail-suspension mice. In addition, AX treatment mitigated the generation of mitochondrial ROS, cytochrome c release into the cytosol, and caspase 3 activation in Sol8 myotubes.

Although the body weight of mice decreased after tail suspension, EDL muscle weight did not influence this reduction. This meant that muscle atrophy induced by tail suspension was not due to decreased body weight stemming from starvation. Indeed, numerous studies demonstrate that the weight loss in EDL is hardly detectable in suspended animals [31,32]. Consistent with these findings, tail suspension induced a loss of skeletal muscle, including the GA, TA, and SO, but not the EDL muscle (Figure 2-2). Although GA and TA are mostly composed of fast-twitch fibers, they also contain intermediate muscle fibers such as IIa (GA: 20.9% ± 1.6%, TA: 18.2% ± 2.4%). In contrast, EDL is occupied by fast-twitch fibers such as IIb. Indeed, we found that the size of IIa in muscle fibers in the S-ND group showed significantly decreased, compared with the C-ND group in the SO muscle (Figure 2-2). Thus, muscle atrophy caused by tail suspension preferentially affected slow-type rather than fast-type muscles. Moreover, AX prevented atrophy in the muscle containing type I and IIa myofibers. These findings suggest that AX acts in slow-twitch and intermediate muscle fibers.

The CSA of type I and IIa myofibers in S-AX group significantly increased, compared with S-CN or other groups (Figure 2-3). SO muscle contains type IIx (11.8% ± 1.7%) and type IIb (3.1% ± 1.1%) as well as type I (30.6% ± 1.2%), type IIa (49.1% ± 1.2%) [21]. Given the influence of AX in type I and IIa muscle fibers, AX is likely to contribute to the transformation of type IIx to type I and IIa in SO muscle of tail-suspension mice, indicating increased CSA in S-AX. Likewise, TA muscle contains type IIx (44.7% ± 11.9%, CSA: 2186.0 ± 35.2 μm^2), type I (0.6% ± 1.6%, CSA: 1501.4 ± 7.1 μm^2) and type IIa (18.2% ± 2.4%, CSA: 1369.6 ± 22.4 μm^2). Additionally, GA muscle contains type IIx (19.6% ± 2.1%, CSA: 2186.0 ± 35.2 μm^2), type I (7.9% ± 0.5%, CSA: 1743.4 ± 28.2 μm^2) and type IIa (41.6% ± 1.3%, CSA: 1346.2 ± 22.8 μm^2) [21]. We found that the wet weight of TA and GA in the C-AX group was significantly decreased, compared with C-ND group. AX is presumed to cause the transformation of type IIx to type I and IIa muscle fibers, resulting in the shift to small-sized fibers. However, further studies are necessary to define this mechanism.

We found that the ratio of body weight/food intake decreased significantly at 5 and 6 weeks in the tail-suspension group (S-ND and S-AX). Previous studies showed that there was an increased reliance on carbohydrate metabolism for energy associated with muscle unloading [33]. In addition, shift of fiber phenotype was related to the downregulation of mitochondrial proteins and upregulation of glycolytic protein, suggesting a shift from oxidative to glycolytic metabolism [26]. Consistent with these results, we found the decreased ratio of body weight/food intake and the shift of type fibers caused by tail suspension. Additionally, we found that the mRNA expression of oxidative metabolism-related transcription factors was decreased in the tail-suspension group. Thus, these results showed that the decreased ratio of body

weight/food intake was associated with the energy shift from oxidative to glycolytic metabolism.

Numerous studies have demonstrated that mitochondria play an important role in muscle atrophy [5,7,8,34,35]. In oxidative phosphorylation, mitochondrial respiratory chain complexes I and III are believed to be the major sites of ROS leakage, although other components of oxidative phosphorylation also contribute to the production of ROS in the mitochondria [36,37]. In this study, we found that the amount of H_2O_2 production was significantly increased by tail suspension in normal diet mice (S-ND group). However, the AX-supplemented diet inhibited the increase of H_2O_2 production in the S-AX group. In addition, there was a significant reduction in mitochondrial respiratory chain complexes I and III in the SO muscle of the S-ND group, compared to that of the C-ND group (Figure 2-4). Kanazashi et al. reported that the SO muscle displays a decreased succinate dehydrogenase activity, an integral component of the mitochondrial respiratory chain, and increased oxidative stress during hindlimb suspension in rats [19]. Our previous study also demonstrates that mitochondrial dislocation during unloading conditions has deleterious effects on muscle fibers leading to atrophy and ROS leakage from the mitochondria [5]. The weakening of mitochondrial oxidative phosphorylation is usually accompanied with changes in mitochondrial biosynthesis. We found that the expression of energy and oxidative metabolism genes significantly decreased in the SO muscle of tail-suspension mice, while AX showed the regulating effect on the mitochondria biogenesis (Figure 2-6). Therefore, muscle atrophy stimulated by unloading stress in tail suspension is associated with the disturbance of mitochondrial ability including mitochondrial oxidative phosphorylation and mitochondrial biogenesis.

Numerous reports have proven that AX exerts its effects on mitochondria in fatty-liver disease, caused due to a high-fat diet, nonalcoholic steatohepatitis [38,39], gastric inflammation by oxidative stress [40], and cardiovascular diseases [41,42]. These unique characteristics of AX on mitochondria may relate to itself membrane structure. AX consists of conjugated double bonds and hydroxyl and keto groups that can embed in the cell membrane, from the inside to the outside. This feature confers strong antioxidant activity, which enables AX to react with the free radicals [43,44]. Our results indicated that AX was preferentially detected in the mitochondrial fraction and is consistent with previous reports of its accumulation in the mitochondria of normal human mesangial cells and blastocysts [15,30]. These findings strengthened the possibility that AX reacted to ROS produced from mitochondrial respiratory chain complexes, leading to the prevention of oxidative stress-related diseases, including muscle atrophy.

AnA is an inhibitor of the mitochondrial respiratory chain complex III, a major site of mitochondrial ROS generation, and strongly activates the production and release of superoxide anions into the inner mitochondria membrane space [45]. We examined the effect of AX on AnA-induced mitochondrial O_2^- production using succinate as a complex II substrate. AX significantly suppressed mitochondrial complex III-driven ROS production in Sol8 myotubes (Figure 2-7A), whereas its effect was not observed in C2C12 myotubes (data not shown), which is likely to be involved in muscle fiber type. Sol8 and C2C12 cells were derived from SO and adult dystrophic mouse muscles, respectively. Indo et al. showed that the SO muscle, which is enriched with slow-twitch fibers, exhibits a higher production of ROS than fast-twitch fibers [3]. Some studies have also reported that dietary antioxidants reduce ROS production and

ameliorate atrophy in the SO muscle more than other fast-twitch fibers [46-48]. These results indicate that AX could target the mitochondria to eliminate O_2^- production and inhibit muscle atrophy induced by mitochondrial oxidative stress in slow-twitch fibers.

Loss of MMP and excess ROS production in mitochondria leads to cytochrome c release from the mitochondria into the cytosol, resulting in the induction of apoptosis [49-53]. It has been revealed that overproduction of mitochondrial ROS, mitochondrial dysfunction, and mitochondria-mediated apoptosis play vital roles in skeletal muscle atrophy [54,55]. Caspase 3 is downstream of cytochrome c; the release of cytochrome c activates caspase 3, which induces apoptosis [56,57]. It has been reported that a deficiency in caspase 3 prevents denervation-induced muscle atrophy [58]. In addition, disturbed TUNEL-positive nuclei, increased caspase 3 protein level, and decreased Bcl-2, anti-apoptotic members that inhibit the release of cytochrome c by unloading were improved by AX [48]. In our present study, AX showed improvement of disturbed MMP as well as increased mitochondrial ROS by AnA treatment, thereby inactivating caspase 3 through an inhibition of cytochrome c release into cytosol in Sol8 myotubes. In agreement with these findings, AX has been shown to protect against decreased MMP by virtue of improving mitochondrial function in cancer and neural cells [14,59]. These results suggested that AX targeted and protected mitochondria by scavenging free oxygen radicals, regulating MMP, and inhibiting apoptosis in muscle cells.

2.5 Conclusion

In summary, the current study revealed that AX prevented muscle atrophy in slow-type muscles (SO). The direct effect of AX on mitochondria brought about the reduction of oxidative stress, regulation of mitochondrial function such as oxidative phosphorylation, biogenesis and MMP, and attenuation of apoptosis (Figure 2-9). These effects could collectively prevent the onset of muscle atrophy. Based on these results, AX could be considered as a potential treatment option for muscle atrophy and mitochondria-related diseases.

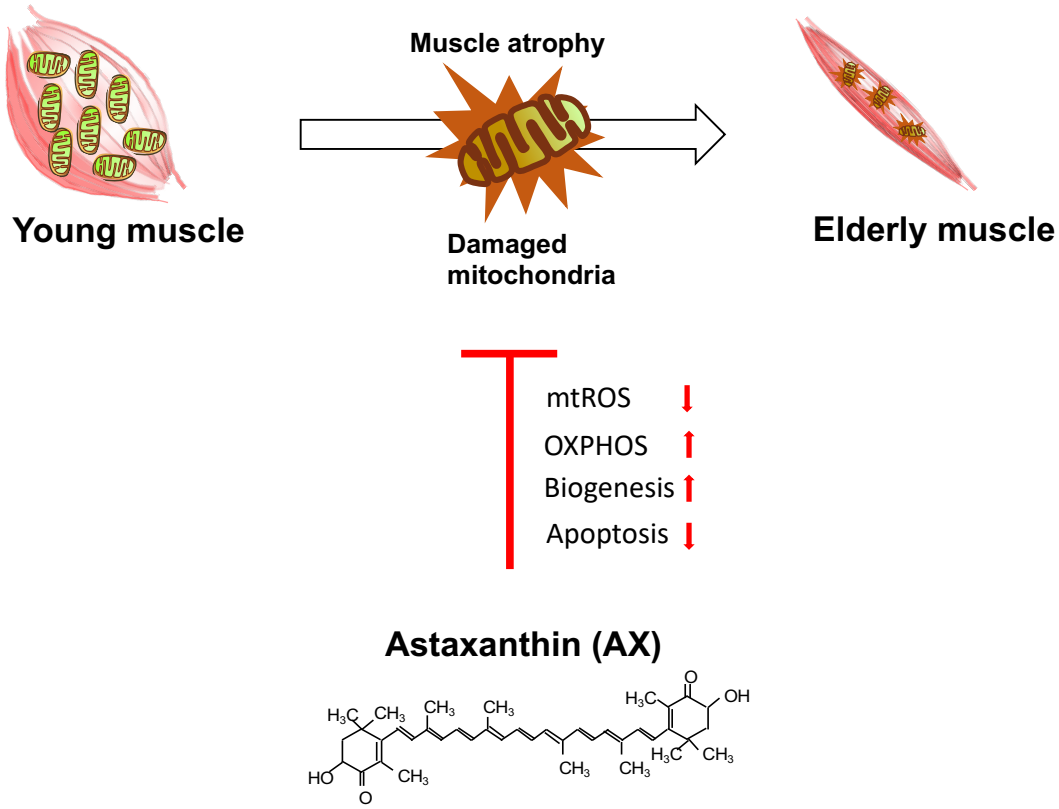

Figure 2-9. The proposed mechanisms of AX on muscle atrophy which caused by mitochondrial dysfunction. mtROS, mitochondrial reactive oxygen species; OXPHOS, oxidative phosphorylation.

2.6 References

[1] Goto, K.; Okuyama, R.; Honda, M.; Uchida, H.; Akema, T.; Ohira, Y.; Yoshioka, T. Profiles of Connectin (Titin) in Atrophied Soleus Muscle Induced by Unloading of Rats. *J. Appl. Physiol.* 2003, *94*, 897-902.

[2] Ohira, Y. Neuromuscular Adaptation to Microgravity Environment. *Jpn. J. Physiol*. 2000, *50*, 303-314.

[3] Mishra, P.; Varuzhanyan, G.; Pham, A.H.; Chan, D.C. Mitochondrial dynamics is a distinguishing feature of skeletal muscle fiber types and regulates organellar compartmentalization. *Cell Metab.* 2007, *7*, 106-118.

[4] Chance, B.; Sies, H.; Boveris, A. Hydroperoxide Metabolism in Mammalian Organs. *Physiol. Rev.* 1979, *59*, 527-605.

[5] Nikawa, T.; Ishidoh, K.; Hirasaka, K.; Ishihara, I.; Ikemoto, M.; Kano, M.; Kominami, E.; Nonaka, I.; Ogawa, T.; Adams, G.R.; et al. Skeletal Muscle Gene Expression in Space-Flown Rats. *FASEB J.* 2004, *18*, 522-524.

[6] Powers, S.K.; Smuder, A.J.; Criswell, D.S. Mechanistic Links between Oxidative Stress and Disuse Muscle Atrophy. *Antioxid. Redox Signal.* 2011, *15*, 2519-2528.

[7] Romanello, V.; Guadagnin, E.; Gomes, L.; Roder, I.; Sandri, C.; Petersen, Y.; Milan, G.; Masiero, E.; Del, P.P.; Foretz, M.; et al. Mitochondrial fission and remodelling contributes to muscle atrophy. *EMBO J.* 2010, *29*, 1774-1785.

[8] Adhihetty, P.L.; Ljubicic, V.; Menzies, K.J.; Hood, D.A. Differential susceptibility of subsarcolemmal and intermyofibrillar mitochondria to apoptotic stimuli. *Am. J. Physiol. Cell Physiol.* 2005, *289*, C994-C1001.

[9] Kowaltowski, A.J.; Vercesi, A.E. Mitochondrial damage induced by conditions of oxidative stress. *Free Radic. Biol. Med.* 1999, *26*, 463-471.

[10] Davinelli, S.; Nielsen, M.E.; Scapagnini, G. Astaxanthin in Skin Health, Repair, and Disease: A Comprehensive Review. *Nutrients* 2018, *10*, 522.

[11] Yuan, J.P.; Peng, J.; Yin, K.; Wang, J.H. Potential Health-Promoting Effects of Astaxanthin: A High-Value Carotenoid Mostly from Microalgae. *Mol. Nutr. Food Res.* 2011, *55*, 150-165.

[12] Ohno, M.; Darwish, W.S.; Ikenaka, Y.; Miki, W.; Ishizuka, M. Astaxanthin Can Alter CYP1A-dependent Activities via Two Different Mechanisms: Induction of Protein Expression and Inhibition of NADPH P450 Reductase Dependent Electron Transfer. *Food Chem. Toxicol.* 2011, *49*, 1285-1291.

[13] Wolf, A.M.; Asoh, S.; Hiranuma, H.; Ohsawa, I.; Iio, K.; Satou, A.; Ishikura, M.; Ohta, S. Astaxanthin Protects Mitochondrial Redox State and Functional Integrity Against Oxidative Stress. *J. Nutr. Biochem.* 2010, *21*, 381-389.

[14] Zhang, Z.W.; Xu, X.C.; Liu, T.; Yuan, S. Mitochondrion-Permeable Antioxidants to Treat ROS-Burst-Mediated Acute Diseases. *Oxid. Med. Cell Longev.* 2016, *1*, 6859523.

[15] Kuroki, T.; Ikeda, S.; Okada, T.; Maoka, T.; Kitamura, A.; Sugimoto, M.; Kume, S. Astaxanthin Ameliorates Heat Stress-Induced Impairment of Blastocyst Development in Vitro: Astaxanthin Colocalization with and Action on Mitochondria. *J. Assist. Reprod. Genet.* 2013, *30*, 623-631.

[16] Song, X.D.; Wang, B.S.; Lin, S.C.; Jing, L.L.; Mao, C.P.; Xu, P.; Lv, C.J.; Liu, W.; Zuo, J. Astaxanthin Inhibits Apoptosis in Alveolar Epithelial Cells Type II in Vivo and in

Vitro Through the ROS-dependent Mitochondrial Signalling Pathway. *J. Cell. Mol. Med.* 2014, *18*, 2198-2212.

[17] Mukai, R.; Matsui, N.; Fujikura, Y.; Matsumoto, N.; Hou, D.X.; Kanzaki, N.; Shibata, H.; Horikawa, M.; Iwasa, K.; Hirasaka, K.; et al. Preventive Effect of Dietary Quercetin on Disuse Muscle Atrophy by Targeting Mitochondria in Denervated Mice. *J. Nutr. Biochem.* 2016, *31*, 67-76.

[18] Hiramoto, S.; Yahata, N.; Saitoh, K.; Yoshimura, T.; Wang, Y.; Taniyama, S.; Nikawa, T.; Tachibana, K.; Hirasaka, K. Dietary Supplementation with Alkylresorcinols Prevents Muscle Atrophy Through a Shift of Energy Supply. *J. Nutr. Biochem.* 2018, *61*, 147-154.

[19] Kanazashi, M.; Tanaka, M.; Nakanishi, Y.; Maeshige, N.; Fujino, H. Effects of Astaxanthin Supplementation and Electrical Stimulation on Muscle Atrophy and Decreased Oxidative Capacity in Soleus Muscle During Hindlimb Unloading in Rats. *J. Physiol. Sci.* 2019, *69*, 757-767.

[20] Shibaguchi, T.; Yamaguchi, Y.; Miyaji, N.; Yoshihara, T.; Naito, H.; Goto, K.; Ohmori, D.; Yoshioka, T.; Sugiura, T. Astaxanthin Intake Attenuates Muscle Atrophy Caused by Immobilization in Rats. *Physiol. Rep.* 2016, *4*, e12885.

[21] Bloemberg, D.; Quadrilatero, J. Rapid Determination of Myosin Heavy Chain Expression in Rat, Mouse, and Human Skeletal Muscle Using Multicolor Immunofluorescence Analysis. *PLoS ONE* 2012, *7*, e35273.

[22] Kim, M.J.; Hwang, S.H.; Lim, J.A.; Froehner, S.C.; Adams, M.E.; Kim, H.S. alpha-syntrophin modulates myogenin expression in differentiating myoblasts. *PLoS ONE* 2010, *5*, e15355.

[23] Sprague, J.E.; Yang, X.M.; Sommers, J.; Gilman, T.L.; Mills, E.M. Roles of Norepinephrine, Free Fatty Acids, Thyroid Status, and Skeletal Muscle Uncoupling Protein 3 Expression in Sympathomimetic-Induced Thermogenesis. *J. Pharmacol. Exp. Ther.* 2007, *320*, 274-280.

[24] Hirasaka, K.; Lago, C.U.; Kenaston, M.A.; Fathe, K.; Nowinski, S.M.; Nikawa, T.; Mills, E.M. Identification of a Redox-Modulatory Interaction Between Uncoupling Protein 3 and Thioredoxin 2 in the Mitochondrial Intermembrane Space. *Antioxid. Redox Signal.* 2011, *15*, 2645-2661.

[25] Hirasaka, K.; Saito, S.; Yamaguchi, S.; Miyazaki, R.; Wang, Y.; Haruna, M.; Taniyama, S.; Higashitani, A.; Terao, J.; Nikawa, T.; et al. Dietary supplementation with Isoflavones Prevents Muscle Wasting in Tumor-Bearing Mice. *J. Nutr. Sci. Vitaminol.* 2016, *62*, 178-184.

[26] Ohira, T.; Ohira, T.; Kawano, F.; Shibaguchi, T.; Okabe, H.; Goto, K.; Ogita, F.; Sudoh, M.; Roy, R.R.; Edgerton, V.R.; et al. Effects of gravitational loading levels on protein expression related to metabolic and/or morphologic properties of mouse neck muscles. *Physiol. Rep.* 2014, *2*, e00183.

[27] Kitaoka, Y.; Takeda, K.; Tamura, Y.; Fujimaki, S.; Takemasa, T.; Hatta, H. Nrf2 Deficiency Does Not Affect Denervation-Induced Alterations in Mitochondrial Fission and Fusion Proteins in Skeletal Muscle. *Physiol. Rep.* 2016, *4*, e13064.

[28] Yeo, D.; Ji, L.L. Mitochondrial dysfunction and muscle disuse atrophy. *F1000Research* 2019, *8*, 1621.

[29] Nishida, Y.; Nawaz, A.; Kado, T.; Takikawa, A.; Igarashi, Y.; Onogi, Y.; Wada, T.; Sasaoka, T.; Yamamoto, S.; Sasahara, M.; et al. Astaxanthin stimulates mitochondrial biogenesis in insulin resistant muscle via activation of AMPK pathway. *J. Cachexia Sarcopenia Muscle* 2020, *11*, 241-258.

[30] Manabe, E.; Handa, O.; Naito, Y.; Mizushima, K.; Akagiri, S.; Adachi, S.; Takagi, T.; Kokura, S.; Maoka, T.; Yoshikawa, T. Astaxanthin Protects Mesangial Cells from Hyperglycemia-Induced Oxidative Signaling. *J. Cell. Biochem.* 2008, *103*, 1925-1937.

[31] Musacchia, X.J.; Steffen, J.M.; Deavers, D.R. Rat Hindlimb Muscle Responses to Suspension Hypokinesia/Hypodynamia. *Aviat. Space Environ. Med.* 1983, *54*, 1015-1020.

[32] Desplanches, D.; Mayet, M.H.; Sempore, B.; Flandrois, R. Structural and Functional Responses to Prolonged Hindlimb Suspension in Rat Muscle. *J. Appl. Physiol.* 1987, *63*, 558-563.

[33] Stein, T.P.; Schluter, M.D.; Galante, A.T.; Soteropoulos, P.; Ramirez, M.; Bigbee, A.; Grindeland, R.E.; Wade, C.E. Effect of hind limb muscle unloading on liver metabolism of rats. *J. Nutr. Biochem.* 2005, *16*, 9-16.

[34] Marzetti, E.; Hwang, J.C.Y.; Lees, H.A.; Wohlgemuth, S.E.; Dupont-Versteegden, E.E.; Carter, C.S.; Bernabei, R.; Leeuwenburgh, C. Mitochondrial Death Effectors: Relevance to Sarcopenia and Disuse Muscle Atrophy. *Biochim. Biophys. Acta* 2010, *1800*, 235-244.

[35] Romanello, V.; Sandri, M. Mitochondrial Biogenesis and Fragmentation as Regulators of Protein Degradation in Striated Muscles. *J. Mol. Cell. Cardiol.* 2013, *55*, 64-72.

[36] Brand, M.D. The Sites and Topology of Mitochondrial Superoxide Production. *Exp. Gerontol.* 2010, *45*, 466-472.

[37] Choi, M.H.; Ow, J.R.; Yang, N.D.; Taneja, R. Oxidative Stress-Mediated Skeletal Muscle Degeneration: Molecules, Mechanisms, and Therapies. *Oxid. Med. Cell. Longev.* 2016, 6842568.

[38] Bhuvaneswari, S.; Anuradha, C.V. Astaxanthin Prevents Loss of Insulin Signaling and Improves Glucose Metabolism in Liver of Insulin Resistant Mice. *Can. J. Physiol. Pharmacol.* 2012, *90*, 1544-1552.

[39] Ni, Y.; Nagashimada, M.; Zhuge, F.; Zhan, L.L.; Nagata, N.; Tsutsui, A.; Nakanuma, Y.; Kaneko, S.; Ota, T. Astaxanthin Prevents and Reverses Diet-Induced Insulin Resistance and Steatohepatitis in Mice: A Comparison with Vitamin E. *Sci. Rep.* 2015, *5*, 17192.

[40] Kim, S.H.; Lim, J.W.; Kim, H. Astaxanthin Inhibits Mitochondrial Dysfunction and Interleukin-8 Expression in *Helicobacter pylori*-Infected Gastric Epithelial Cells. *Nutrients* 2018, *10*, 1320.

[41] Fan, C.D.; Sun, J.Y.; Fu, X.T.; Hou, Y.J.; Li, Y.; Yang, M.F.; Fu, X.Y.; Sun, B.Y. Astaxanthin Attenuates Homocysteine-Induced Cardiotoxicity in Vitro and in Vivo by Inhibiting Mitochondrial Dysfunction and Oxidative Damage. *Front. Physiol.* 2017, *8*, 1041.

[42] Krestinina, O.; Baburina, Y.; Krestinin, R.; Odinokova, I.; Fadeeva, I.; Sotnikova, L. Astaxanthin Prevents Mitochondrial Impairment Induced by Isoproterenol in Isolated Rat Heart Mitochondria. *Antioxidants* 2020, *9*, 262.

[43] Higuera-Ciapara, I.; Félix-Valenzuela, L.; Goycoolea, F.M. Astaxanthin: A Review of Its Chemistry and Applications. *Crit. Rev. Food Sci. Nutr.* 2006, *46*, 185-196.

[44] Ambati, R.R.; Phang, S.M.; Ravi, S.; Aswathanarayana, R.G. Astaxanthin: Sources, Extraction, Stability, Biological Activities and Its Commercial Applications—A Review. *Mar. Drugs* 2014, *12*, 128-152.

[45] Turrens, J.F.; Alexandre, A.; Lehninger, A.L. Ubisemiquinone Is the Electron Donor for Superoxide Formation by Complex III of Heart Mitochondria. *Arch. Biochem. Biophys.* 1985, *237*, 408-414.

[46] Kitakaze, T.; Harada, N.; Imagita, H.; Yamaji, R. β-Carotene Increases Muscle Mass and Hypertrophy in the Soleus Muscle in Mice. *J. Nutr. Sci. Vitaminol.* 2015, *61*, 481-487.

[47] Ogawa, M.; Kariya, Y.; Kitakaze, T.; Yamaji, R.; Harada, N.; Sakamoto, T.; Hosotani, K.; Nakano, Y.; Inui, H. The Preventive Effect of β-Carotene on Denervation-Induced Soleus Muscle Atrophy in Mice. *Br. J. Nutr.* 2013, *109*, 1349-1358.

[48] Yoshihara, T.; Yamamoto, Y.; Shibaguchi, T.; Miyaji, N.; Kakigi, R.; Naito, H.; Goto, K.; Ohmori, D.; Yoshioka, T.; Sugiura, T. Dietary Astaxanthin Supplementation Attenuates Disuse-Induced Muscle Atrophy and Myonuclear Apoptosis in the Rat Soleus Muscle. *J. Physiol. Sci.* 2017, *67*, 181-190.

[49] Li, J.; Yu, W.; Li, X.T.; Qi, S.H.; Li, B. The Effects of Propofol on Mitochondrial Dysfunction Following Focal Cerebral Ischemia-Reperfusion in Rats. *Neuropharmacology* 2014, *77*, 358-368.

[50] He, G.D.; Feng, C.; Vinothkumar, R.; Chen, W.Q.; Dai, X.X.; Chen, X.; Ye, Q.Q.; Qiu, C.Y.; Zhou, H.P.; Wang, Y.; et al. Curcumin Analog EF24 Induces Apoptosis via ROS-dependent Mitochondrial Dysfunction in Human Colorectal Cancer Cells. *Cancer Chemother. Pharmacol.* 2016, *78*, 1151-1161.

[51] Shanmugapriya, K.; Kim, H.; Kang, H.W. In Vitro Antitumor Potential of Astaxanthin Nanoemulsion Against Cancer Cells via Mitochondrial Mediated Apoptosis. *Int. J. Pharm.* 2019, *560*, 334-346.

[52] Pajaniradje, S.; Mohankumar, K.; Pamidimukkala, R.; Subramanian, S.; Rajagopalan, R. Antiproliferative and Apoptotic Effects of Sesbania Grandiflora Leaves in Human Cancer Cells. *BioMed Res. Int.* 2014, 474953.

[53] Meghani, N.; Patel, P.; Kansara, K.; Ranjan, S.; Dasgupta, N.; Ramalingam, C.; Kumar, A. Formulation of Vitamin D Encapsulated Cinnamon Oil Nanoemulsion: Its Potential Anti-Cancerous Activity in Human Alveolar Carcinoma Cells. *Colloids Surf. B Biointerfaces* 2018, *166*, 349-357.

[54] Du, J.; Wang, X.N.; Miereles, C.; Bailey, J.L.; Debigare, R.; Zheng, B.; Price, S.R.; Mitch, W.E. Activation of caspase-3 Is an Initial Step Triggering Accelerated Muscle Proteolysis in Catabolic Conditions. *J. Clin. Investig.* 2004, *113*, 115-123.

[55] Powers, S.K.; Kavazis, A.N.; McClung, J.M. Oxidative Stress and Disuse Muscle Atrophy. *J. Appl. Physiol.* 2007, *102*, 2389-2397.

[56] Wu, Q.; Tang, Z.H.; Peng, J.; Liao, L.; Pan, L.H.; Wu, C.Y.; Jiang, Z.S.; Wang, G.X.; Liu, L.S. The Dual Behavior of PCSK9 in the Regulation of Apoptosis Is Crucial in Alzheimer's Disease Progression (Review). *Biomed. Rep.* 2014, *2*, 167-171.

[57] Yang, Q.S.; Guo, S.F.; Wang, S.; Qian, Y.W.; Tai, H.P.; Chen, Z.X. Advanced Glycation End Products-Induced Chondrocyte Apoptosis Through Mitochondrial Dysfunction in Cultured Rabbit Chondrocyte. *Fundam. Clin. Pharmacol.* 2015, *29*, 54-61.

[58] Plant, P.J.; Bain, J.R.; Correa, J.E.; Woo, M.; Batt, J. Absence of caspase-3 Protects Against Denervation-Induced Skeletal Muscle Atrophy. *J. Appl. Physiol.* 2009, *107*, 224-234.

[59] Liu, X.B.; Shibata, T.; Hisaka, S.; Osawa, T. Astaxanthin Inhibits Reactive Oxygen Species-Mediated Cellular Toxicity in Dopamin- ergic SH-SY5Y Cells via Mitochondria-Targeted Protective Mechanism. *Brain Res.* 2009, *1254*, 18-27.

Abbreviations

AMPK	adenosine 5'-monophosphate-activated protein kinase
AnA	antimycin A
ATP	adenosine triphosphate
AX	astaxanthin
BCA	bicinchoninic acid
CCCP	cytochrome cyanide m-chlorophenyl
CSA	cross-sectional area
DHE	dihydroethidium
DMEM	Dulbecco's modified Eagle medium
DMSO	dimethyl sulfoxide
EDL	extensor digitorum longus
EDTA	ethylenediaminetetraacetic acid
FBS	fetal bovine serum
GA	gastrocnemius
GAPDH	glyceraldehyde 3-phosphate dehydrogenase
HBSS	Hank's balanced salt solutions
H_2O_2	hydrogen peroxide
HPLC	High-performance liquid chromatography
HS	horse serum
MHC	myosin heavy chain
MMP	mitochondrial membrane potential
MOPS	3-(N-morpholino) propanesulfonic acid
Ndufa	NADH: ubiquinone oxidoreductase complex assembly factor
OXPHOS	oxidative phosphorylation
PPAR	peroxisome proliferator-activated receptor
PVDF	polyvinylidene difluoride
ROS	reactive oxygen species
Sdhb	succinate dehydrogenase complex, subunit B
SDS-PAGE	sodium dodecyl sulfate-polyacrylamide gel electrophoresis
SO	soleus
TA	tibialis anterior
UCP	uncoupling protein

Chapter III

The effect of AX on immune disorder induced by mitochondrial dysfunction

3.1 Introduction

The immune system is an important system for the body to trigger immune responses and perform the necessary functions. The immune system consists of organs (bone marrow, spleen, lymph nodes, etc.), immune cells (phagocytes, lymphocytes, etc.), and immunologically active substances (lysozyme, leukocytes interferon, interleukin, etc.). Macrophages, a member of phagocytes, are allosteric, and the variations of their phenotype and function are influenced by different factors, especially by the surrounding microenvironment [1,2]. Commonly, macrophages are polarized into different subtypes such as M1 and M2 macrophages, depending on the changes in the environment. M1 (classical) macrophages (e.g., lipopolysaccharide (LPS) stimulation) usually exhibit a pro-inflammatory response and release large amounts of pro-inflammatory cytokines, such as tumor necrosis factor (TNF)-α, interleukin (IL)-1β, inducible nitric oxide synthase (iNOS), and monocyte chemoattractant protein (MCP)-1. On the other hand, M2 (alternative) macrophages (e.g., IL-4 / IL-13 stimulation) usually exhibit an anti-inflammatory response and repair function [3]. In infected tissues or organs, macrophages are primarily polarized to M1 phenotype, displaying the pro-inflammatory function to help the host resist pathogens. Subsequently, in order to avoid the excessive damage of pro-inflammatory factors to the host, macrophages are polarized to M2 phenotype to drive an anti-inflammatory response and repair damaged tissues or organs [2]. Thus, modulation of immune function is carried out by regulating macrophage polarization, leading to maintained homeostasis.

Mitochondria have long been known as the energy factories. Metabolites are oxidized through the tricarboxylic acid (TCA) cycle in the mitochondrial matrix and then pass through the electron transport chain (ETC) in the inner membrane of mitochondria to produce

adenosine-triphosphate (ATP). Recently, mitochondria are being considered an energy source for immunity in addition to being the powerhouses of the cell [4]. With the special status of mitochondria as the central hub of metabolism, they are necessary to maintain and establish the immune cell phenotypes [5]. Similarly, mitochondrial metabolism modulates the biological activity and functions of macrophages [6]. The modification of mitochondrial metabolism and physiological function, such as mitochondrial reactive oxygen species (mtROS), mitochondrial membrane potential (MMP), mitochondrial DNA (mtDNA), mitochondrial oxidative phosphorylation (OXPHOS), TCA cycle, and mitochondrial ultrastructure are crucial indicators of macrophage activation and polarization [7-10]. In addition, remodeling of mitochondrial metabolism in macrophages is regarded as an anti-inflammatory signal [11]. Recently, targeting mitochondria to meliorate inflammatory diseases by regulating mitochondrial metabolism has become possible.

In recent years, AX is being studied for mitochondria-related diseases due to its unique structure and activity. AX reportedly maintains mitochondrial integrity by reducing oxidative stress, prevents the loss of MMP, and increases mitochondrial oxygen consumption which inhibits mitochondrial dysfunction [12-14]. In my previous study, I also found that AX was easily accumulated in the mitochondria of muscle cells rather than in the cytosol and prevented mitochondrial disorder-induced muscle atrophy by regulating mitochondrial function [15]. Moreover, not only due to its antioxidant activity, but AX's anti-inflammatory activity also plays a role in many chronic and acute diseases such as neurological diseases, diabetes, gastrointestinal diseases, hepatic and renal diseases, skin and eye disorders [16]. Although the mechanisms of anti-inflammatory activity of AX have been partially investigated, a large part

of the mechanisms is still unknown. And, crucially, the details of many of the identified anti-inflammatory mechanisms and whether there are some cross-talks between different signaling pathways still deserve further exploration. Hence, we investigated the anti-inflammatory effects of AX on LPS-stimulated RAW264.7 cells and the mechanisms of AX acted on mitochondrial metabolism under the M1 macrophages. A specific effect of AX on succinate dehydrogenase (SDH, an important enzyme on mitochondria) and a regulatory effect on the SDH-HIF-1α axis of AX which is partially involved in the anti-inflammatory mechanisms of AX were proposed. Remarkably, AX reprogrammed mitochondrial metabolism and suppressed a shift from an OXPHOS phenotype to a glycolytic phenotype during M1 macrophage polarization.

3.2 Materials and methods

3.2.1 Cell culture and treatment

RAW264.7 cells were obtained from the American Type Culture Collection (Rockville, MD, USA). They were cultured in Dulbecco's modified Eagle medium (DMEM; D5796, Sigma-Aldrich, St. Louis, MO, USA)) supplemented with 10% fetal bovine serum (FBS; 12483020, Gibco, Grand Island, NY, USA), 10,000 units/mL penicillin-streptomycin (15140122, Gibco, Grand Island, NY, USA) and maintained at 37 °C in a 5% CO_2. Cells were harvested and seeded in dishes for 24 h for the attachment and until treatment.

AX was purchased from Sigma-Aldrich, (SML0982, Sigma-Aldrich) and prepared in dimethyl sulfoxide (DMSO; 04524511, Fujifilm Wako Pure Chemical Corporation, Osaka, Japan). LPS from *Escherichia coli* O111:B4 was purchased from Sigma-Aldrich, (L4391, Sigma-Aldrich) and prepared in PBS (-) (16623555, Fujifilm Wako Pure Chemical

Corporation). Cells were treated with AX (10 μM) / DMSO for 24 h, then followed with the LPS (1 μg/mL) / PBS (-) stimulation for indicated time with a daily medium change.

3.2.2 Quantitative real-time polymerase chain reaction (qRT-PCR)

Total RNA was extracted from cells using an acid guanidinium thiocyanate-phenol-chloroform mixture (ISOGEN^{TM}; Nippon Gene, Tokyo, Japan). Reverse transcription for cDNA synthesis and qRT-PCR analysis were performed with the appropriate primers and SYBR Green dye using a real-time PCR system (ABI Real-Time PCR Detection System; Applied Biosystems, Foster City, CA, USA), as described previously [15]. The mRNA levels were normalized to the housekeeping gene *18S* ribosomal RNA. The oligonucleotide primers used for PCR are shown as Table 3-1.

3.2.3 Enzyme-linked immunosorbent assay (ELISA)

For the detection of released IL-1β, ELISA (R&D Systems, Inc (Minneapolis, MN)) was performed following the manufacturer's instructions. Briefly, cell culture supernatants were collected and centrifuged at 12,000 rpm at 4 °C for 5 min, and supernatants were acquired for detection. The collected supernatants were added into microplate wells which were coated with assay diluent RD1N (R&D Systems, 895488) for 2 h incubation at room temperature (RT). Free unbound reactants were removed by aspirating and washing. After the last wash, the remaining wash buffer was removed, followed by incubation with mouse IL-1β conjugate (R&D Systems, 893830) for 2 h, RT. The preceding washing step was repeated, and the substrate solution was added and incubated (mixture of color A reagent and color B reagent with a ratio of 1:1) for 30

min, RT, protected from light. The absorbance at 450 nm was measured by a microplate reader (BioTek Cytation 3, Winooski, VT, USA).

Table 3-1. The oligonucleotide primers and sequence.

Target gene		Sequence
Tnf-α	F	5'- GGCCTCCCTCTCATCAGTTC -3'
	R	5'- CTTTGAGATCCATGCCGTTG -3'
Il-6	F	5'- CCGGAGAGGAGACTTCACAG -3'
	R	5'- TCCACGATTTCCCAGAGAAC -3'
Il-1b	F	5'- CTCATCTGGGATCCTCTCCA -3'
	R	5'- GGGTCCGTCAACTTCAAAGA -3'
Sdhb	F	5'- GGAGGGCAAGCAACAGTATC -3'
	R	5'- CTTGTCTCCGTTCCACCAGT -3'
18S	F	5'- CCATCCAATCGGTAGTAGCG -3'
	R	5'- GTAACCCGTTG-AACCCCATT -3'

F, forward primer; R, reversed primer; *Tnf*, tumor necrosis factor; *Il*, interleukin; *Sdhb*, succinate dehydrogenase complex, subunit B; *18S*, 18S ribosomal RNA.

3.2.4 Mitochondrial superoxide levels measurement

The superoxide production from mitochondria was detected using MitoSOX Red fluorescent probe, Invitrogen, as described by the protocol. Cells were harvested and seeded in a black 96-well plate with a density of 5×10^4 cells/well, AX (10 μM) / DMSO were treated for 24 h, then LPS (1 μg/mL)-stimulated for 6 h with fresh media. After that, cells were washed

by warm HBSS and incubated with 5 μM MitoSOX reagent (M36008, Thermo Fisher Scientific) for 30 min at 37 °C, protected from light. Fluorescence was recorded using a microplate reader (BioTek Cytation 3) at excitation and emission wavelengths of 490 nm and 595 nm, respectively.

3.2.5 Mitochondrial membrane potential (MMP) measurement

For MMP measurement, the pre-treatment of AX and stimulation of LPS were consistent with mitochondrial superoxide production measurement. After that, cells were washed with PBS and incubated with 1.5 μM JC-1 dye (Thermo Fisher Scientific) for 30 min at 37 °C, protected from light. Fluorescence was recorded using a microplate reader (BioTek Cytation 3) at 550 nm excitation / 600 nm emission and 485 nm excitation / 535 nm emission wavelengths, respectively.

3.2.6 Protein extraction and Immunoblotting

RAW264.7 cells were prepared in Lysis buffer containing 50 mM Tris-HCl, pH 7.5, 150 mM NaCl, 1% Triton X-100, 5 mM EDTA, 10 mM NaF, 2 mM Na_3VO_4, and a protease inhibitor cocktail tablet without EDTA (Roche Diagnostics, Indianapolis, IN, USA) and homogenized using a sonicator. The Pierce BCA assay (Pierce, Rochford, IL, USA) was used to quantify proteins. Protein samples were combined with 4× sample buffer (250 mM Tris-HCl, 8% SDS, 40% glycerol, 8% beta-mercaptoethanol, and 0.02% bromophenol blue) and subjected to SDS-PAGE. The proteins were transferred onto a polyvinylidene difluoride (PVDF) membrane and probed with primary antibodies according to the manufacturer's instructions.

Anti-Total OXPHOS (Abcam, ab110413, Cambridge, UK), anti-HIF-1α (NB100-449, Novus, USA), and anti-β-actin (GTX629630, AC-15, Gene Tex, Irvine, CA, USA) were used. Donkey anti-rabbit IgG (NA934V, GE Healthcare, Little Chalfont, UK) at 1:5000 and sheep anti-mouse IgG (NAX931, GE Healthcare) at 1:5,000 were used as the secondary antibodies. Membranes were developed using ImmunoStar® Zeta Western blotting detection reagents (Fujifilm Wako Pure Chemical Corporation). Immunocomplexes on the membrane were analyzed by Image J software (National Institutes of Health, Bethesda, MD, USA).

3.2.7 Succinate dehydrogenase (SDH) activity assay

The activity of SDH was detected by using a colorimetric method according to the manufacturer's guidelines. Briefly, 1×10^6 cells/sample were homogenized with 100 μL ice-cold SDH assay buffer, then centrifuged at 10,000 ×*g* for 5 min, 4 °C. The supernatants were collected in new tubes. The supernatant was diluted with SDH assay buffer, then 50 μL dilution of supernatant was loaded in each well of the 96-well plate. Subsequently, 50 μL SDH reaction mix (SDH assay buffer 46 μL, SDH probe 2 μL, and SDH substrate mix 2 μL) was added to each well to make a final volume of 100 μL per well. The absorbance was measured at a wavelength of 600 nm for 30 min with an interval every 3 min.

3.2.8 Extracellular flux analysis

The oxygen consumption rates (OCRs) and the extracellular acidification rates (ECAR) were measured using the XFe96 Extracellular Flux Analyzer (Seahorse Bioscience, North Billerica, MA, USA), modified as the previous report [17]. Cells were plated at 4×10^4 cells/well

on a 96-well Seahorse cell culture plate and incubated overnight in growth medium. Then, cells were treated with AX (10 μM) for 24 h and stimulated with LPS (1 μg/mL) for 3 h. For hydrating the cartridge, a sensor cartridge was prepared 24 h before Seahorse XFe96 operation. The sensor cartridge was lowered onto the utility plate and submerged in the sterilization water (200 μL/well) in a non-CO_2 incubator at 37 °C overnight.

For OCRs detection, on the operation day, after 3 h stimulation of LPS, the cell culture medium was removed from the cells and replaced with XF DMEM medium (supplemented with 10 mM glucose, 1 mM pyruvate, and 2 mM L-glutamine), and the cell culture plate was sited in a non-CO_2 incubator at 37 °C for 1 h. Additionally, the sterilization water was removed and discarded from the utility plate, then, replaced with the pre-warmed XF Calibrant (200 μL/well). The assembled sensor cartridge with the utility plate was placed in a non-CO_2 incubator at 37 °C for 1 h prior to loading the injection ports of the sensor cartridge. The OCRs were detected under basal conditions and after the application of 1.5 μM oligomycin to measure the ATP-related oxygen consumption, 2 μM carbonyl cyanide 4-trifluoromethoxy phenylhydrazone (FCCP) to measure the maximum respiratory capacity, and 1 μM rotenone + 1 μM antimycin A to measure the non-mitochondrial oxygen consumption.

For ECARs detection, on the operation day, after 3 h stimulation of LPS, cell culture medium was removed from the cells and replaced with XF DMEM medium (supplemented with 2 mM L-glutamine), and the cell culture plate was sited in non-CO_2 incubator at 37 °C for 1 h. Additionally, the sterilization water was removed and discarded from the utility plate, then replaced with the pre-warmed XF Calibrant (200 μL/well). The assembled sensor cartridge with utility plate was placed in a non-CO_2 incubator at 37 °C for 1 h prior to loading the injection

ports of the sensor cartridge. The ECARs were detected under basal conditions and after the application of 10 mM glucose to measure the glycolysis, 1 μM oligomycin to measure the glycolytic capacity, and 50 mM 2-deoxy-glucose (2-DG) to measure the glycolytic reserve.

After completion of the OCR and ECAR detection, the cells were washed with PBS once and lysed in lysis buffer. The lysates were centrifuged to obtain the protein supernatants, and the protein concentration was detected by BCA assay. The OCR and ECAR values were normalized by the protein concentration and presented as pmol/min/μg protein and mpH/min/μg protein.

3.2.9 Statistical analysis

All data were analyzed by one-way/two-way analysis of variance (ANOVA), using SPSS statistics software, followed by the Tukey or Tukey Kramer (for unequal number) test for individual differences between groups. *p*-values <0.05 were considered to indicate significant differences.

3.3 Results

3.3.1 Effect of AX on the mRNA expression and secretion of cytokines in LPS-stimulated RAW264.7 cells

LPS, a gram-negative bacterial product, infects cells and induces inflammation, which is characterized by the release of pro-inflammatory cytokines such as IL-1β, TNF-α, and IL-6. AX has been known to have an anti-inflammatory effect *in vivo* and *in vitro*. However, the modulation of different pro-inflammatory cytokines also implies different mechanisms

involved in anti-inflammation. To investigate the influence of AX on LPS-stimulated RAW264.7 cells, we measured the mRNA expression of pro-inflammatory cytokines by qRT-PCR and secretion of pro-inflammatory cytokines by ELISA. Consistent with previous studies [18,19], the mRNA expression and secretion of IL-1β, TNF-α, and IL-6 were increased significantly due to the stimulation of LPS (Figure 3-1A, B; TNF-α, IL-6 data not shown). On the contrary, AX downregulated the expression and secretion of these pro-inflammatory cytokines, especially in IL-1β (Figure 3-1A, B; TNF-α, IL-6 data not shown). These results displayed the anti-inflammatory effect of AX, suggesting that AX may play an anti-inflammatory role by inhibiting IL-1β through a specific signaling pathway.

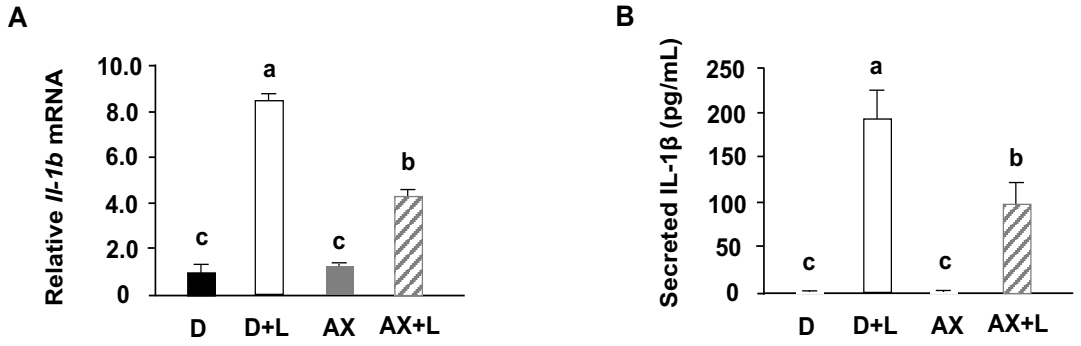

Figure 3-1. Astaxanthin attenuates the mRNA expression and secretion of IL-1β in LPS-stimulated RAW264.7 cells. RAW264.7 cells were in the presence or absence of AX (10 μM) before stimulated with the LPS (1 μg/mL) / PBS (-) for 6 h (A) or 24 h (B). (A) qRT-PCR analysis of *Il-1b* mRNA level. The total RNA of the cells was extracted and subjected to qRT-PCR. Expression ratio is relative to that of *18S*. (B) ELISA analysis of IL-1β secreted level. Supernatants of medium were collected for ELISA detection. Data are represented as mean ± S.D. (A, n=6; B, n=3). Different letters indicate significant differences ($p < 0.05$) based on the one-way ANOVA and Tukey's test. D, DMSO+PBS (-) group; D+L, DMSO+LPS group; AX, Astaxanthin+PBS (-) group; AX+LPS, Astaxanthin+LPS group.

3.3.2 Effect of AX on mitochondrial O_2^- production in LPS-stimulated RAW264.7 cells

Excessive superoxide production by mitochondria is usually thought to be a partial source of inflammation and a catalyst for accelerated inflammation. The excessive ROS production is accompanied by mitochondrial dysfunction, which features a decrease of MMP, disturbance of mitochondrial respiration complex, and so on. In this study, to investigate whether the anti-inflammatory effect of AX is associated with mitochondrial function, we first analyzed the effect of AX on mitochondrial O_2^- production MitoSOX. Mitochondrial O_2^- production in the LPS stimulated group (D+L) was significantly increased, compared with that in the control group (D). In contrast, the addition of AX alleviated mitochondrial O_2^- production in the AX+LPS group (Figure 3-2A).

3.3.3 Effect of AX on MMP in LPS-stimulated RAW264.7 cells

Next, we analyzed the effect of AX on MMP by JC-1 dye. Likewise, MMP in D+L was significantly decreased, compared with that in D. Treatment of AX prevented the decrease of MMP due to LPS stimulation, and maintained higher MMP levels (Figure 3-2B). These results revealed that LPS-induced inflammation is associated with the alteration of mitochondrial O_2^- production and MMP, while AX played a regulatory role on mitochondrial O_2^- production and MMP in LPS-stimulated RAW264.7 cells.

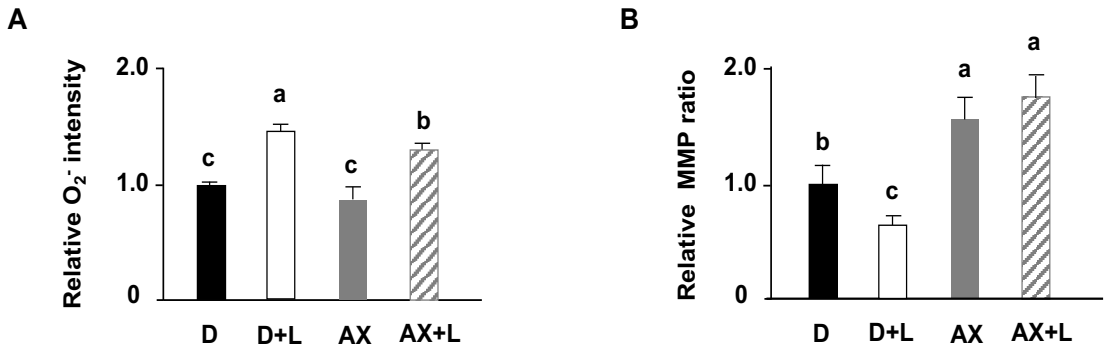

Figure 3-2. Astaxanthin alleviates mitochondrial O_2^- production and maintains MMP in LPS-stimulated RAW264.7 cells. RAW264.7 cells were in the presence or absence of AX (10 μM) before stimulated with the LPS (1 μg/mL) / PBS (-) for 6 h. (A) MitoSOX detection of mitochondrial O_2^- production. (B) JC-1 dye detection of MMP. Data are represented as mean ± S.D. (A and B, n=6). Different letters indicate significant differences ($p < 0.05$) based on the one-way ANOVA and Tukey's test. D, DMSO+PBS (-) group; D+L, DMSO+LPS group; AX, Astaxanthin+PBS (-) group; AX+LPS, Astaxanthin+LPS group.

3.3.4 Effect of AX on mitochondrial complex protein level in LPS-stimulated RAW264.7cells

Mitochondrial respiratory complexes play a vital role in mitochondrial function. Meanwhile, changes in the phenotype, function, and even energy metabolism of macrophages are accompanied by the variation of mitochondrial respiratory complexes in a certain sense. To further study the effect of AX on mitochondria in LPS-stimulated RAW264.7 cells, we examined the alteration of mitochondrial respiratory complexes by immunoblotting. The amounts of mitochondrial respiratory complexes I, II, III, and IV proteins in the D+L group were significantly decreased, compared with those in the D group. Interestingly, we found that AX prevented the reduction of mitochondrial respiratory complexes I, II, and III, but not IV, which was caused by LPS stimulation (Figure 3-3A, B). In particular, mitochondrial respiratory complex II, succinate dehydrogenase subunit B (SDHB), is an important complex protein on the mitochondrial electron transport chain (ETC) as well as an essential enzyme in the tricarboxylic acid cycle (TCA cycle), as it is the connection point of ETC and TCA cycle, and critical for the inflammatory response.

3.3.5 Effect of AX on mitochondrial SDH activity and *Sdhb* gene level in LPS-stimulated RAW264.7 cells

Based on these results, we continued to investigate the effect of AX on the activity of SDH and the mRNA level of *Sdhb*. In accordance with the findings of protein expression, AX prevented the reduction of SDH activity (Figure 3-3C). Furthermore, treatment of AX improved the decrease of *Sdhb* mRNA expression by LPS stimulation (Figure 3-3D). These results

demonstrated that AX has a regulatory effect on mitochondrial respiratory complex proteins in LPS-stimulated RAW264.7 cells.

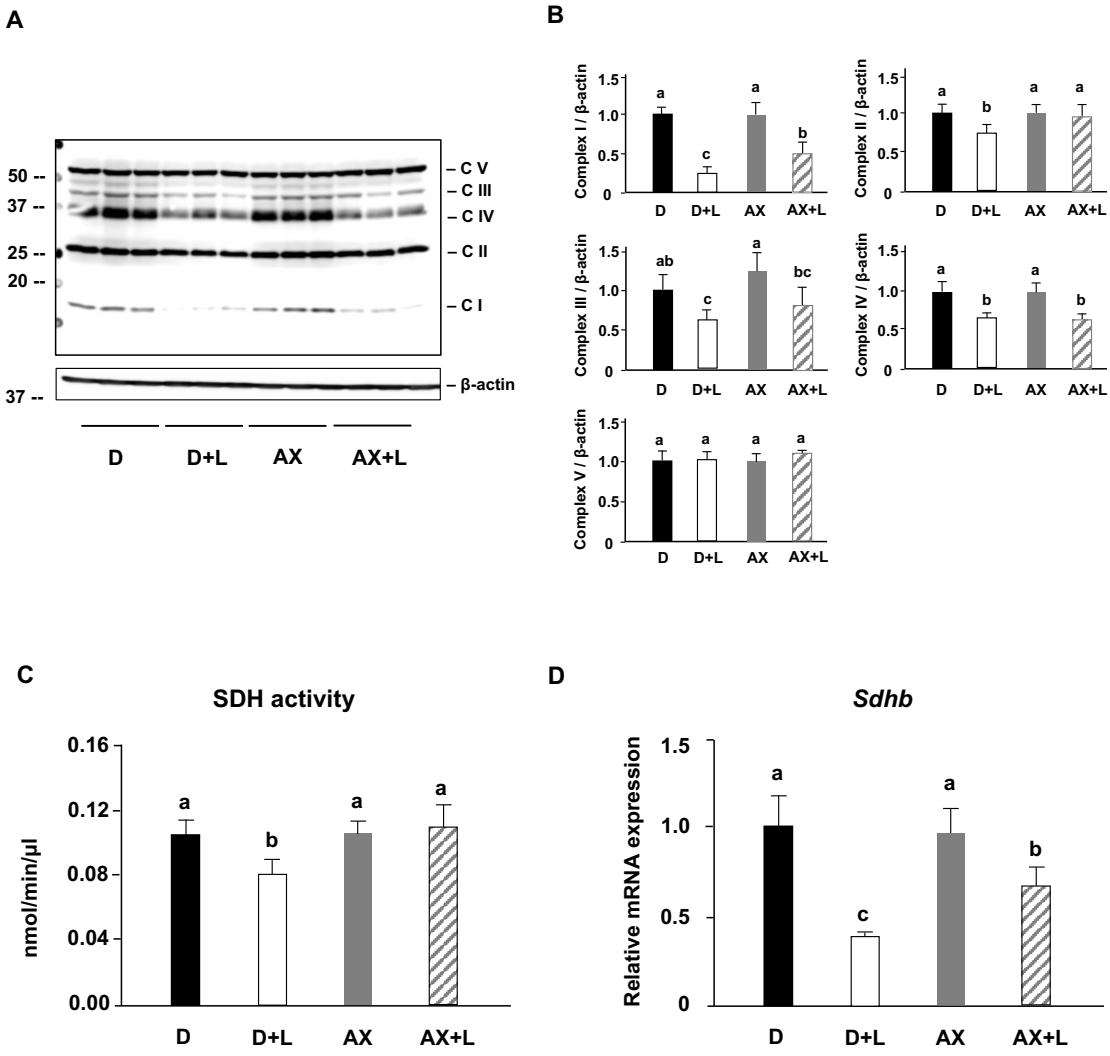

Figure 3-3. Astaxanthin prevents the reduction of SDH activity and up-regulates the protein and mRNA level of *Sdhb* in LPS-stimulated RAW 264.7 cells. RAW 264.7 cells were in the presence or absence of AX (10 μM) before stimulated with the LPS (1 μg/mL) / PBS (-) for 6 h (D) or 24 h (A) (C). (A) Western blot analysis of total OXPHOS proteins and β-actin. (B) Quantification of (A). NADH dehydrogenase beta subcomplex subunit 8 of Complex I (NDUFB8), succinate dehydrogenase subunit B of Complex II (SDHB), cytochrome b-c1 complex subunit 2 of Complex III (UQCRC2), cytochrome c oxidase subunit 1 of Complex IV (MTCO1), and ATP synthase subunit alpha of Complex V (ATP5A). (C) Succinate dehydrogenase (SDH) activity assay. (D) *Sdhb* mRNA expression. Expression ratio is relative to that of *18S*. Data are represented as mean ± S.D. (A and B, n=3; C, n=4; D, n=6). Different letters indicate significant differences ($p < 0.05$) based on the one-way ANOVA and Tukey's test. D, DMSO+PBS (-) group; D+L, DMSO+LPS group; AX, Astaxanthin+PBS (-) group; AX+LPS, Astaxanthin+LPS group.

3.3.6 Effect of AX on HIF-1α level in LPS-stimulated RAW264.7 cells

During classical M1 macrophage activation, alterations in certain mitochondrial metabolites are regarded as an inflammatory signal-inducing cytokine (such as IL-1β) release through HIF-1α [20]. To investigate whether HIF-1α plays a role in LPS-stimulated RAW264.7 cells and the effect of AX on the HIF-1α, we detected the protein expression of HIF-1α in LPS-stimulated RAW264.7 cells. Interestingly, the HIF-1α protein level was upregulated by LPS significantly (Figure 3-4A, B). In contrast, AX downregulated the HIF-1α protein expression caused by LPS stimulation.

3.3.7 Effect of AX on HIF-1α-induced the IL-1β in LPS-stimulated RAW264.7 cells

Subsequently, to confirm whether AX affects the mitochondria-mediated HIF-1α signaling pathway, we used atpenin A5 (AA5), a kind of inhibitor of SDH. Although the co-treatment of LPS and AA5 significantly decreased the *Sdhb* mRNA level, AX pretreatment did not improve its expression completely (Figure 3-4C). Moreover, the addition of AA5 abrogated the original downregulation of IL-1β (Figure 3-4D) and HIF-1α (Figure 3-4E, F) by AX. These results demonstrated that AX blocked the IL-1β expression by regulating the upstream of SDH-HIF-1α axis.

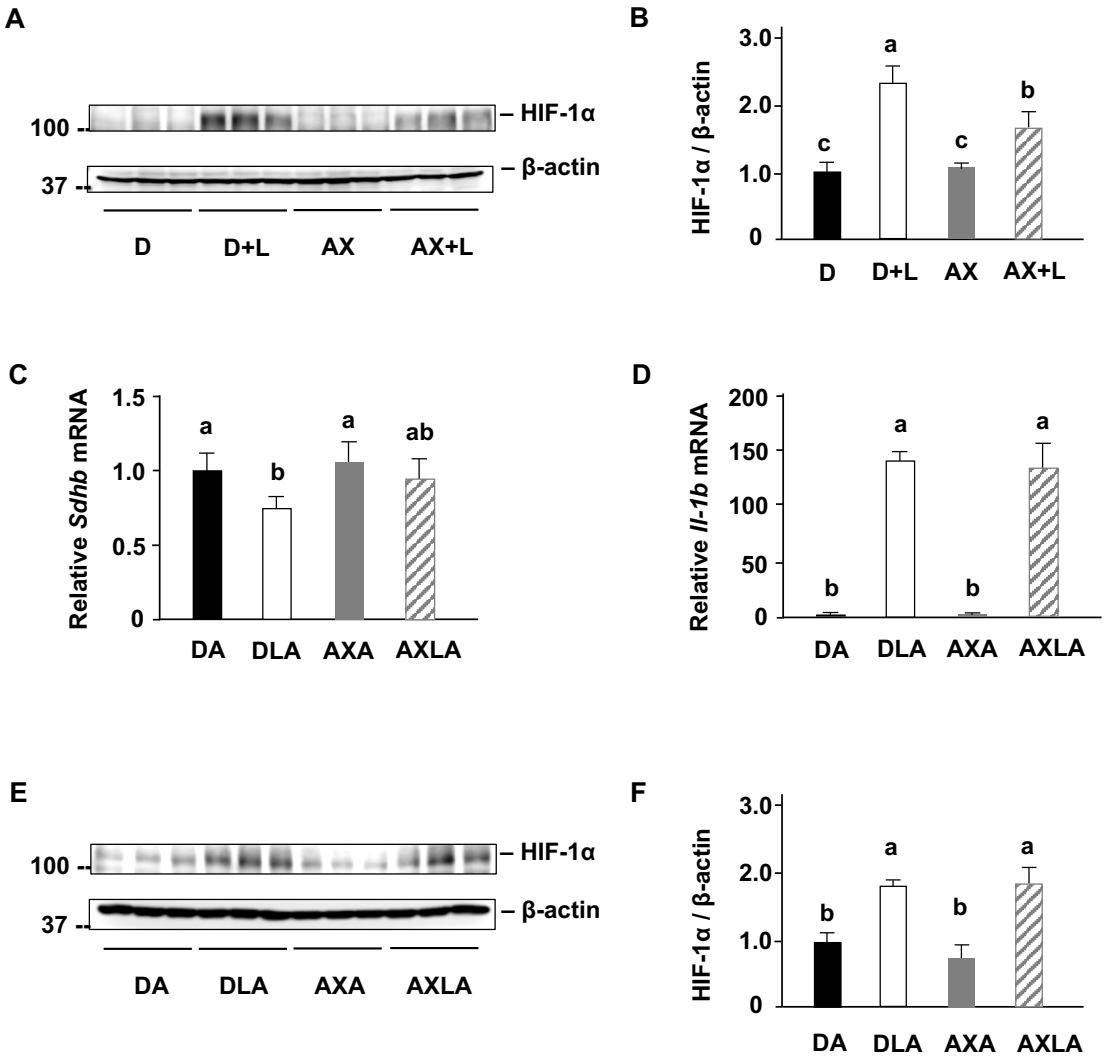

Figure 3-4. Astaxanthin blocks the IL-1β expression by regulating SDH- HIF-1α axis in LPS-stimulated RAW264.7 cells. (A) Western blot analysis of HIF-1α and β-actin. RAW264.7 cells were in the presence or absence of AX (10 μM) before stimulated with the LPS (1 μg/mL) / PBS (-) for 24 h. (B) Quantification of (A). (C) *Sdhb* mRNA expression. (D) *Il-1b* mRNA expression. Expression ratio is relative to that of *18S*. (E) Western blot analysis of HIF-1α and β-actin. (F) Quantification of (E). (C-F) RAW264.7 cells were in the presence or absence of AX (10 μM) before stimulated with LPS (1 μg/mL) / PBS (-) for 3 h (C) (D) or 20 h (E) (F), then atpenin A5 (AA5) was added and treated for a further 4 h together with LPS. Data are represented as mean ± S.D. (B, n=3; C and D, n=6; F, n=3). Different letters indicate significant differences ($p < 0.05$) based on the one-way ANOVA and Tukey's test. D, DMSO+PBS (-) group; D+L, DMSO+LPS group; DA, DMSO+AA5 group; DLA, DMSO+LPS+AA5 group; AX, Astaxanthin+PBS (-) group; AX+LPS, Astaxanthin+LPS group; AXA, AX+AA5 group; AXLA, AX+LPS+AA5 group.

3.3.8 Effect of AX on mitochondrial energy metabolism shift in LPS-stimulated RAW264.7 cells

Numerous studies showed that LPS stimulation induces a shift towards a glycolytic phenotype. To investigate whether AX has an effect on mitochondrial metabolism and the phenotype of AX in LPS-stimulated RAW264.7 cells, we measured key parameters of mitochondrial function by directly measuring the oxygen consumption rate (OCR) and glycolytic function by directly measuring the extracellular acidification rate (ECAR) of cells.

For OCR, as shown in Figure 3-5A, B (no injection), the basal level of OCRs (OCR before oligomycin - OCR after Rot/AnA) were D: 213.32 ± 34.54 pmol/min/μg protein, D+L: 190.27 ± 35.50 pmol/min/μg protein, AX: 223.93 ± 40.14 pmol/min/μg protein and AX+L: 212.24 ± 46.83 pmol/min/μg protein. In comparison to the D group, the D+L group had a slightly lower basal OCR, although it was not significant. AX group tended to maintain a higher basal OCR compared with the D group. There were no significant differences between the AX+LPS group and other groups. Subsequently, oligomycin, as an inhibitor of ATP synthase (complex V), was injected. It impacted or decreased electron flow through the ETC, resulting in a reduction in mitochondrial respiration or OCR. This decrease in OCR was linked to cellular ATP production. Through the decreased OCR (Figure 3-5A, B (oligomycin +)), we found that under the condition of oligomycin injection, the D+L group showed a great reduction and significant difference to the D group in ATP-linked respiration OCR level (OCR before oligomycin – OCR after oligomycin). However, the ATP-linked respiration OCR level in the AX group and even in the AX+LPS group showed no significant differences to the D group (D: 165.20 ± 23.569 pmol/min/μg protein, D+L: 135.02 ± 21.28 pmol/min/μg protein, AX: 167.50 ± 34.02

pmol/min/μg protein and AX+L: 169.04 ± 37.07 pmol/min/μg protein). FCCP (carbonyl cyanide-4 (trifluoromethoxy) phenylhydrazone), an uncoupling agent, was the 2nd injection following oligomycin. As a result, electron flow through the ETC was uninhibited, and oxygen consumption by complex IV reached its maximum. As shown in Figure 3-5A, B (FCCP +), compared to the maximum respiration OCR (OCR after FCCP - OCR after Rot/AnA) of the D group (D: 532.46 ± 84.32 pmol/min/μg protein), the D+L group showed a significant decrease (D+L: 423.34 ± 79.67 pmol/min/μg protein). However, there were no significant differences between the AX group (516.89 ± 54.36 pmol/min/μg protein), the AX+L group (478.69 ± 20.04 pmol/min/μg protein), and the D group. The mixture of Rot/AnA, an inhibitor of mitochondrial complexes I and III, was the 3rd and final injection. This combination stopped mitochondrial respiration and enabled the calculation of nonmitochondrial respiration driven by processes outside of the mitochondria. As shown in Figure 3-5A, B (Rot/AnA +), there were no significant changes among the D group (75.05 ± 11.84 pmol/min/mg/ml protein), the D+L group (71.10 ± 14.60 pmol/min/mg/ml protein), the AX group (76.35 ± 6.25 pmol/min/mg/ml protein), and the AX+L group (75.18 ± 11.52 pmol/min/mg/ml protein). These results revealed that AX saved mitochondrial respiratory function and contributed particularly to maintaining the ATP production-related respiration and maximum respiration capacity in LPS-stimulated RAW264.7 cells.

For ECAR, the first injection was a saturated concentration of glucose (Figure 3-5C). The injected glucose was used by cells and metabolized into pyruvate with the production of ATP, NADH, water, and protons through the glycolytic pathway. The extrusion of protons into the surrounding medium resulted in a rapid increase in ECAR. This glucose-induced response

was reported as the rate of glycolysis under basal conditions. As shown in Figure 3-5C, D (glucose +), treatment of LPS resulted in a significant increase in glycolysis rate (ECAR after glucose - ECAR before glucose, 156.70 ± 49.85 mpH/min/μg protein) compared to the D group (77.80 ± 24.30 mpH/min/μg protein). Nevertheless, the AX+LPS group (80.40 ± 33.55 mpH/min/μg protein) suppressed the upregulation of glycolysis rate which was caused by LPS, and showed no significant differences between the D group and the AX group (89.60 ± 27.90 mpH/min/μg protein). Moreover, following the injection of oligomycin, energy production was shifted to the glycolysis process, and the subsequent increase in ECAR revealed the cellular maximal glycolytic capacity. We found that not only basal glycolysis rate but also maximum glycolytic capacity was noticeably increased in the D+LPS group (200.06 ± 47.59 mpH/min/μg l protein) compared to the D group (126.36 ± 47.59 mpH/min/μg protein), while the AX+LPS group (101.30 ± 41.80 mpH/min/μg protein) maintained similar maximum glycolytic capacity level to the D group and the AX group (140.02 ± 34.09 mpH/min/μg protein). These results demonstrated that although the stimulation of LPS increased the glycolytic rate and maximum glycolytic capacity, AX pre-treatment maintained a relatively stable glycolytic rate and maximum glycolytic capacity in the cells and remained nearly identical to unstimulated cells.

To further elaborate on the cell energy phenotype, we displayed differential metabolic parafmeters (Mitochondrial respiration related: Basal respiration, ATP production, Maximum respiration; Glycolytic function related: Glycolysis rate, Maximum glycolytic capacity) in Figure 3-5E. Apparently, compared to the D group, the D+L group showed a relative decrease in mitochondrial respiratory function accompanied by a significant increase in glycolytic capacity. However, the AX+LPS group kept a stable mitochondrial respiratory function and lo-

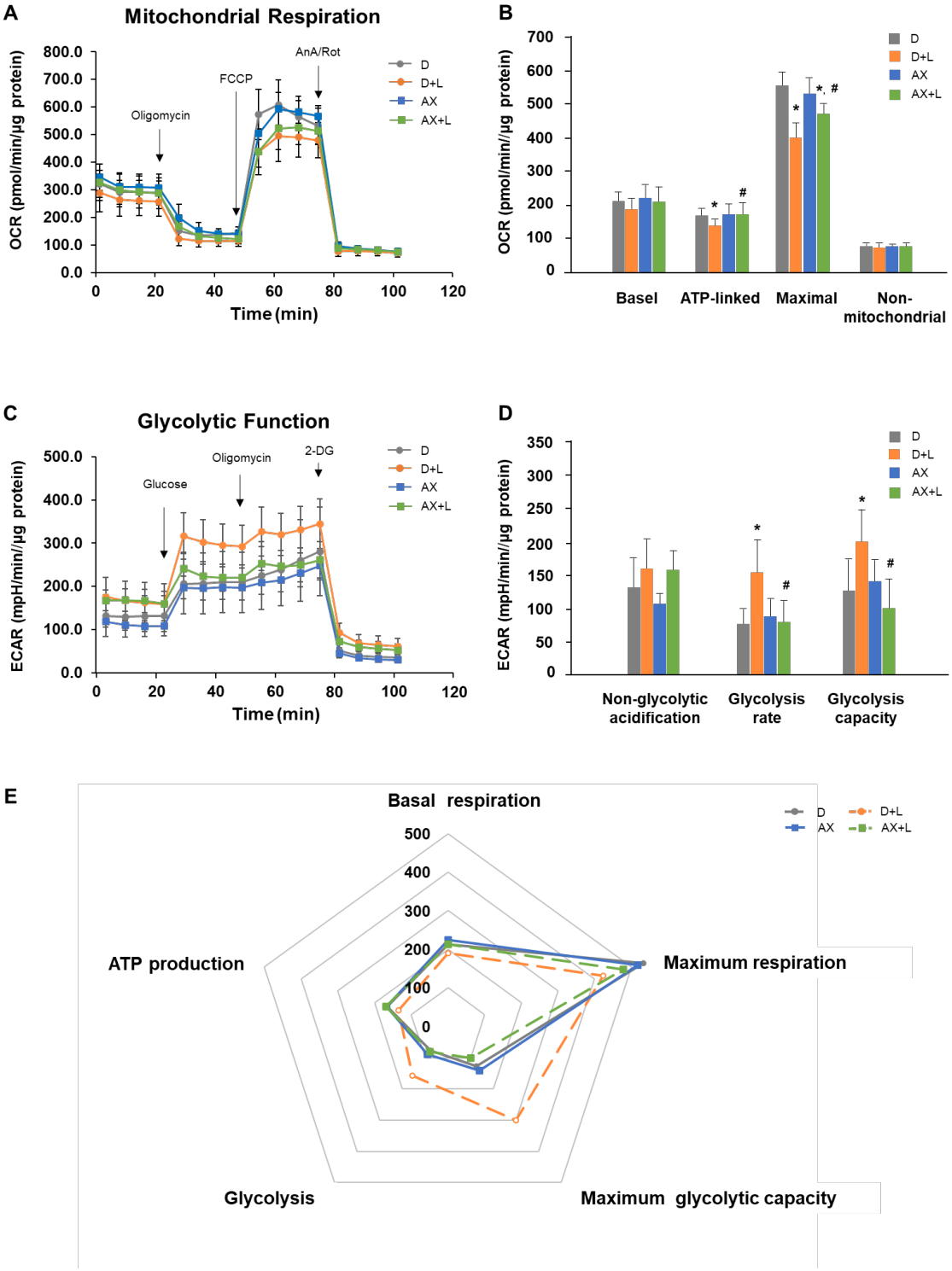
A
Mitochondrial Respiration
OCR (pmol/min/μg protein)
Time (min)
Oligomycin
FCCP
AnA/Rot
D
D+L
AX
AX+L
B
OCR (pmol/min//μg protein)
Basel
ATP-linked
Maximal
Non-mitochondrial
C
Glycolytic Function
ECAR (mpH/min//μg protein)
Glucose
Oligomycin
2-DG
D
Time (min)
D
AX
AX+L
D
ECAR (mpH/min//μg protein)
Non-glycolytic acidification
Glycolysis rate
Glycolysis capacity
E
Basal respiration
ATP production
Maximum respiration
Glycolysis
Maximum glycolytic capacity
D
D+L
AX
AX+L

Figure 3-5. Astaxanthin suppresses a shift from an OXPHOS phenotype towards a glycolytic phenotype in LPS-stimulated RAW264.7 cells. RAW264.7 cells were in the presence or absence of AX (10 μM) before stimulated with the LPS (1 μg/mL) / PBS (-) for 3 h. During extracellular flux analysis, cells were treated with (A) oligomycin, FCCP, AnA/Rot to detect the mitochondrial respiration according to the OCRs levels or treated with (C) glucose, oligomycin, 2-DG to detect the glycolytic function according to the ECARs levels. (B) Basal respiration, mitochondrial ATP-linked respiration, maximum respiration, and non-mitochondrial respiration were calculated based on OCRs levels. (D) Non-glycolytic acidification, glycolysis rate, and maximum glycolysis capacity were calculated based on ECARs. (E) Both calculated OXPHOS and glycolysis metabolic parameters were displayed in summary. Data are represented as mean ± S.D. (n≥12). Different letters indicate significant differences ($p < 0.05$) based on the one-way ANOVA and Tukey's or Tukey Kuramar's test. FCCP, carbonyl cyanide-4 (trifluoromethoxy) phenylhydrazone; AnA/Rot, Antimycin A/Rotenone; 2-DG, 2-deoxyglucose. D, DMSO+PBS (-) group; D+L, DMSO+LPS group; AX, Astaxanthin+PBS (-) group; AX+LPS, Astaxanthin+LPS group.

wer glycolysis. Overall, AX suppressed a shift from an OXPHOS phenotype towards a glycolytic phenotype in LPS-stimulated RAW264.7 cells.

3.4 Discussion

The novel findings of this part revealed the following: AX exerted immunomodulatory effects by reprogramming mitochondrial metabolism, AX suppressed a shift from an OXPHOS phenotype towards a glycolytic phenotype, and AX prevented HIF-1α induced IL-1β by regulating SDH activity and expression (a graphical illustration is shown in Figure 3-6).

Consistent with previous studies, LPS stimulation led to the release of a large number of pro-inflammatory cytokines in RAW264.7 macrophage cells [18] while AX effectively inhibited the release of these pro-inflammatory cytokines, especially in IL-1β (Figure 3-1A, B). Although it has been reported that AX suppressed IL-1β expression by blocking the nuclear translocation of NF-κB p65 subunit and IκBα in LPS-stimulated RAW264.7 cells [20], existing results raised our curiosity about whether AX regulates IL-1β in a unique rather than a single way, such as in an inflammasome-dependent manner or in a way regulated by mitochondria. Therefore, we investigated the effects of AX on mitochondria in the immune response.

Reactive oxygen species (ROS) production is considered the central part of the progression of inflammation [21]. It is a partial source of inflammation and a catalyst for accelerated inflammation. ROS derived from mitochondria are produced by ETC through OXPHOS and are viewed as the major source of free radicals [22]. We found that AX had an alleviative effect on mitochondrial ROS production in response to immune response signals (Figure 3-2A). It is

possibly involved in the unique structure of AX. Particularly, the structural property of the long nonpolar conjugated double bonds and the polar groups such as keto and hydroxyl at each end of double bonds enable AX to be embedded in the cell membrane and scavenge ROS in both the inner and outer lipid layers of the cellular membrane [23,24]. Our previous studies supported that AX was more likely to accumulate in mitochondria, which membranes also have a phospholipid backbone similar to the cell membrane structure [15]. Here, we also demonstrated the possibility that AX acts on mitochondria and scavenges mitochondrial free radicals in macrophages. Likewise, the effect of AX on mitochondrial ROS was also found in gastric epithelial cells [25], alveolar epithelial cells type II [26], vascular smooth muscle cells [27], and so on.

The ETC on the mitochondria consists of 2 electron carriers (coenzyme Q [CoQ] and Cyt c), and a range of complexes (I, II, III, IV, V) in the mitochondrial inner membrane [28]. Electron leakage from at least 11 different sites within the mitochondria leads to mtROS [29], and complexes I and III are known as the major sites of ROS generation [30-32]. Complex I produces ROS into the mitochondrial matrix, whereas complex III can produce ROS into either the mitochondrial matrix or intermembrane space [33]. In the mitochondrial immune response, consistent with the result of Aki T and colleagues [34], we also found significant reductions in mitochondrial complexes I, II, III, and IV during LPS stimulation of macrophages and activation into the M1 phenotype (Figure 3-3A, B). These findings indicated the changes in mitochondrial proteins and functions as a result of LPS stimulation, as well as the phenotype changes of mitochondria under M1 macrophages. In our data, for these two primary mtROS-producing sites (complex I and III), AX improved their protein level, especially for complex I

(Figure 3-3A, B). The complex I-derived ROS displayed an important effect on the immune system [28]. One mechanism by which complex I produces large amounts of O_2^- is reverse electron transport (RET), which occurs at a high proton motive force and a reduced coenzyme Q (CoQ) pool [35]. In macrophages, it has been reported that RET-derived ROS induce pro-IL-1β production through a specific signaling pathway [36]. Moreover, the ROS produced from complex I inhibit the IL-10 expression [37] and also oxidize mitochondrial deoxyribonucleic acid (mtDNA) and activate IL-1β [36]. These all suggest clear effects of complex I-derived ROS on the immune response and the important role of maintaining stable complex I expression for immune regulation. Although the specific sites of action of AX in mitochondrial complex I (e.g., assembly of complex I, subunit proteins of complex I, and electron transport involved in complex I) still require further investigation, we are considering that the protection of complex I by AX and stabilization of its normal expression to reduce ROS caused by complex I play a vital role in the immune response of macrophages.

SDH, also known as complex II, is a dehydrogenase on ETC as well as a member of the TCA cycle, and they are located on the matrix side of the mitochondrial inner membrane [38]. Abnormalities of SDH activity, which induce immune diseases, are usually associated with metabolic dysfunction such as the reduced activity of SDHA and SDHB [39]. Inhibition of SDH activity impairs human T cell activation and function [40] and impairs the macrophage's bactericidal activity *in vitro* [41], while maintaining the activity of SDH contributes to the anti-microbial responses [41]. In this study, LPS stimulation destroyed the SDH activity in macrophages, whereas AX completely prevented this damage (Figure 3-3C). The protective effect of SDH (complex II) activity seems like a part of the anti-microbial response of AX.

Moreover, the reduction of SDH expression in macrophages caused by LPS leads to the accumulation of succinate in the mitochondria, and its release into the cytosol and extracellular space is perceived as an inflammation signal [42, 43]. We showed that AX upregulated the decrease of SDH (especially SDHB, one subunit of SDH) mRNA and protein expression significantly which was induced by LPS stimulation (Figure 3-3A, B, D). On one hand, SDH (complex II) as a part of OXPHOS is a site of mitochondrial superoxide production [44] and also a source of electrons that drives RET at complex I [36]. AX sustains the normal expression of SDH (complex II), which in turn prevents the release of ROS caused by SDH (complex II) dysfunction (this includes ROS leaked from SDH (complex II) itself and possibly also from complex I due to RET). On the other hand, as a member of the TCA cycle, SDH catalyzes the oxidation of succinate to fumarate [38]. There are two interruptions in the TCA cycle of M1-polarized macrophages, one of which is the SDH [11]. The interruption of SDH leads to an accumulation of succinate, which stabilizes the transcription factor hypoxia-inducible factor-1α (HIF-1α) and enhances the IL-1β production and inflammation [20, 42]. Interestingly, this succinate-driven inflammation is associated with ROS [45]. Hence, the safeguard of AX on SDH (complex II) secures the function of SDH in the TCA cycle, slows down the stress from SDH (complex II) brought to complex I, and eliminates the ROS they produce through ETC, which is likely a mechanism by which AX keeps mitochondrial and macrophage homeostasis and thus slows down inflammation.

HIF-1α, an important transcription factor, showed a vital regulatory effect on inflammatory macrophage function [46]. Macrophages normally respond to local hypoxia caused by inflammation-mediated upregulation of HIF-1α [47], while it can also be induced

through stimulation, such as by LPS, under normoxic conditions [48, 49]. Overexpression of HIF-1α in macrophages was found to result in the upregulation of M1 markers [50]. Conversely, knockdown of HIF-1α decreased the M1 marker such as IL-1β production [51]. Intriguing, the limitation of SDHB activity caused by augmented electron flux through complex II attracts HIF-1α activation in a ROS-dependent manner [52]. As described in a previous report, the accumulation of succinate stabilizes the HIF-1α and enhances the IL-1β production, resulting in inflammation most probably by the mechanism related to ROS [20]. Analogously, the reduction of mitochondrial ROS caused by complex I can reduce the oxidative effect of LPS on mitochondrial SDH and impair HIF-1α stabilization and IL-1β expression [51]. These illustrate the important role of the collaboration of SDH, ROS, and HIF-1α in the induction of IL-1β. Based on the specific protective effect of AX on SDH, especially SDHB, and the powerful function of clearing mitochondrial free radicals, as well as the significant inhibitory effect on IL-1β, we are highly interested in whether HIF-1α is also regulated by AX in this progress. Astonishingly, AX suppressed the upregulation of HIF-1α (Figure 3-4A, B). Subsequently, AA5 was used to confirm the effect of AX on this progress. AA5 is one of the inhibitors of SDH, and it showed a significant inhibitory effect on SDH activity [51]. In addition, the co-treatment of LPS and AA5 inhibited *Sdhb* expression (Figure 3-4C), while it noticeably promoted HIF-1α (Figure 3-4E, F) and IL-1β (Figure 3-4D) expressions, compared to the treatment with AA5 alone. These results were consistent with the study of Fuhrmann DC and colleagues [51] that showed that the inhibition of SDH stabilizes HIF-1α and promotes IL-1β. However, the addition of AA5 abrogated the original downregulation of IL-1β (Figure 3-4D)

and HIF-1α (Figure 3-4E, F) by AX. These results noted that the modulatory effect of AX on HIF-1α and the SDH-HIF-1α axis are involved in the IL-1β inhibitory mechanism of AX.

In LPS-activated-M1 macrophages, the metabolic shift from an OXPHOS phenotype to a glycolysis phenotype was observed [20]. This metabolic reprogramming of cells toward aerobic glycolysis, similar to cancer cell metabolism, known as the "Warburg effect," was also found in our study (Figure 3-5E). Interestingly, AX suppressed this metabolic shift from OXPHOS towards glycolysis (Figure 3-5E). On one hand, AX controlled the mitochondrial respiration by improving mitochondrial basal, ATP-linked, and maximal OCR (Figure 3-5A, B). Consisten with the results of a previous report [12], the slightly elevated basal OCR in the presence of AX suggested that AX keeps mitochondrial function in a more active state (Figure 3-5B, basal). ATP inhibition is thought to be associated with decreased MMP [53]. LPS damaged the MMP of macrophages (Figure 3-2B), and in subsequent respiration function test, the addition of oligomycin impeded complex V, which made the disrupted MMP in an even more unrecoverable state, while the ATP-linked OCR was even more inhibited (Figure 3-5B, ATP-linked OCR level as unstimulated macrophages even under the stimulation of LPS (Figure 3-5B, ATP-linked). Simply, these regulations of AX on ATP-linked OCR probably occurred by maintaining a higher membrane potential [12]. Protection of the mitochondrial complex, smoothing of the ETC, maintaining of the MMP, and activation of mitochondria all seem to be the reasons why AX protects the mitochondria of macrophages and thus pursues a more stable state and greater maximum respiratory capacity when macrophages are stimulated (Figure 3-5B, maximal). On the other hand, AX inhibited the abnormal enhancement of glycolytic function, especially glycolysis rate and glycolytic capacity, during the activation of M1

macrophages and it could be considered to make them more inclined to an unstimulated energy metabolism phenotype Figure 3-5C, D). The activation and stabilization of HIF-1α decrease mitochondria OCR while increasing glycolysis [54, 55]. This may be activated in both hypoxic conditions and independent of hypoxia manner such as LPS stimulation [21, 56]. Increased HIF-1α is heavily involved in the expression of many important enzymes and genes related to glycolysis such as hexokinase, phosphofructose kinase, pyruvate kinase M, GLUT1, GLUT3, and LDH-A [55]. Therefore, the downregulation of glycolysis of AX seems to be associated with the inhibitory effect on HIF-1α by AX. In summary, AX suppressed the metabolic shift from OXPHOS towards glycolysis, which may be connected to the protective effect on mitochondria and the inhibitory effect on HIF-1α by AX. We propose these hypotheses based on the available results; however, further studies are needed to investigate the exact mechanisms of how AX affects mitochondrial respiratory and glycolytic functions.

3.5 Conclusion

An important regulatory role of AX on the mutation of mitochondrial SDH caused by external stimuli during the polarization of macrophages toward M1 type has been identified. AX inhibited the stabilization of HIF-1α and IL-1β by regulating SDH. Furthermore, AX suppressed the energy shift from an OXPHOS phenotype to a glycolysis phenotype, which was closely related to the protective effect on mitochondria and the inhibitory effect on HIF-1α by AX (Figure 3-6). These findings revealed important effects of AX on mitochondrial enzymes as well as on mitochondrial energy metabolism in the immune response. In addition, it was suggested that AX may play an important role in other diseases caused by SDH mutation and metabolic disorders.

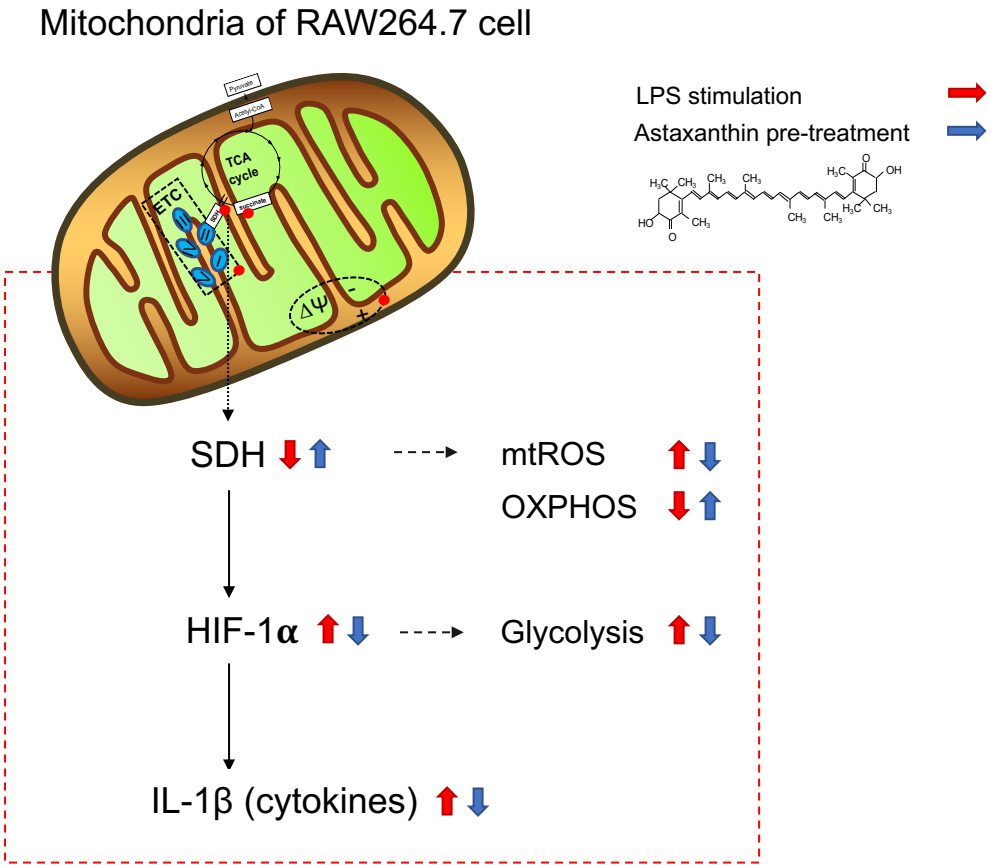

Figure 3-6. The proposed mechanisms of immunomodulatory effect of Astaxanthin. LPS, lipopolysaccharides; TCA cycle, tricarboxylic acid cycle; ETC, electron transport chain; ΔΨ, mitochondrial membrane potential; SDH, succinate dehydrogenase; mtROS, mitochondrial ROS; OXPHOS, oxidative phosphorylation; HIF-1α, hypoxia-inducible factor-1α; IL-β, interleukin-1β.

3.6 References

[1] Shapouri-moghaddam, A.; Mohammandian, S.; Vazini, H.; Taghadosi, M.; Esmaeili, S.A.; Mardani, F.; et al. Macrophage plasticity, polarization, and function in health and disease. *J. Cell Physiol*. 2018, *233*, 6425-6440.

[2] Chen, Y.; Hu, M.; Wang, L.; Chen, W. Macrophage M1/M2 polarization. *Eur. J. Pharmacol.* 2020, *877*, 173090.

[3] Sica, A.; Mantovani, A. Macrophage plasticity and polarization: in vivo veritas. *J. Clin. Invest.* 2012, *122*, 787-795.

[4] Mills, E.L.; Kelly, B.; O'Neil, L.A.J. Mitochondria are the powerhouses of immunity. *Nat. Immunol.* 2017, 18, 488-498.

[5] Weinberg, S.E.; Sena, L.A.; Chandel, N.S. Mitochondria in the regulation of innate and adaptive immunity. *Immunity* 2015, *42*, 406-17.

[6] Langston, P.K.; Shibata, M.; Horng, T. Metabolism supports macrophage activation. *Front Immunol.* 2017, *8*, 61.

[7] Ganeshan, K.; Chawla, A. Metabolic regulation of immune responses. *Annu. Rev. Immunol.* 2014, *32*, 609-34.

[8] EI-Kasmi, K.C.; Stenmark, K.R. Contribution of metabolic reprogramming to macrophage plasticity and function. *Semin. Immunol.* 2015, *27*, 267-275.

[9] Van den Bossche, J.; Baardman, J.; Otto, N.A.; Hoeksema, M.A.; de Vos, A.F.; de Winther, M.P.; et al. Mitochondrial dysfunction prevents repolarization of inflammatory macrophages. *Cell Rep.* 2016, *17*, 684-696.

[10] Wang, Y.; Li, N.; Zhang, X.; Horng, T. Mitochondrial metabolism regulates macrophage biology. *J. Biol. Chem.* 2021, *297*, 100904.

[11] Mills, E.L.; O'Neil, L.A. Reprogramming mitochondrial metabolism in macrophages as an anti-inflammatory signal. *Eur. J. Immunol.* 2016, *46*, 13-21.

[12] Wolf, A.M.; Asoh, S.; Hiranuma, H.; Ohsawa, I.; Iio, K.; Satou, A.; Ishikura, M.; Ohta, S. Astaxanthin Protects Mitochondrial Redox State and Functional Integrity Against Oxidative Stress. *J. Nutr. Biochem.* 2010, *21*, 381–389.

[13] Zhang, Z.W.; Xu, X.C.; Liu, T.; Yuan, S. Mitochondrion-Permeable Antioxidants to Treat ROS-Burst-Mediated Acute Diseases. *Oxid. Med. Cell Longev.* 2016, *2016*, 6859523.

[14] Kuroki, T.; Ikeda, S.; Okada, T.; Maoka, T.; Kitamura, A.; Sugimoto, M.; Kume, S. Astaxanthin ameliorates heat stress-induced impairment of blastocyst development in vitro:--astaxanthin colocalization with and action on mitochondria--. *J. Assist. Reprod. Genet.* 2013, *30*, 623-31.

[15] Sun, L.; Miyaji, N.; Yang, M.; Shi, J.; Tachibana, K.; Hirasaka, K.; et al. Astaxanthin prevents atrophy in slow muscle fibers by inhibiting mitochondrial reactive oxygen species via a mitochondria-mediated apoptosis pathway. *Nutrients* 2021, *13*, 379.

[16] Chang, M.X.; Xiong, F. Astaxanthin and its effects in inflammatory responses and inflammation-associated diseases: recent advances and future directions. *Molecules* 2020, *25*, 5342.

[17] Kim, S.E.; Mori, R.; Komatsu, T.; Chiba, T.; Hayashi, H.; Park, S.; Sugawa, M.D.; Dencher, N.A.; Shimokawa, I. Upregulation of cytochrome c oxidase subunit 6b1 (Cox6b1)

and formation of mitochondrial supercomplexes: implication of Cox6b1 in the effect of calorie restriction. *Age (Dordr)* 2015, *37*, 9787.

[18] Lee, S.J.; Bai, S.K.; Lee, K.S.; Kwon, Y.G.; Lee, S.K.; Kim, Y.M.; et.al. Astaxanthin inhibits nitric oxide production and inflammatory gene expression by suppressing I(kappa)B kinase-dependent NF-kappaB activation. *Mol. Cells* 2003, *16*, 97-105.

[19] Farruggia, C.; Kim, M.B.; Bae, M.; Lee, Y.; Pham, T.X.; Yang, Y.; Han, M.J.; Park, Y.K.; Lee, J.Y. Astaxanthin exerts anti-inflammatory and antioxidant effects in macrophages in NRF2-dependent and independent manners. *J. Nutr. Biochem.* 2018, *62*, 202-209.

[20] Tannahill, G.M.; Curtis, A.M.; Adamik, J.; Auron, P.E.; Xavier, R.J.; O'Neill, L.A.; et al. Succinate is an inflammatory signal that induces IL-1β through HIF-1α. *Nature* 2013, *496*, 238-242.

[21] Mittal, M.; Siddiqui, M.R.; Tran, K.; Reddy, S.P.; Malik, A.B. Reactive oxygen species in inflammation and tissue injury. *Antioxid. Redox Signal* 2014, *20*, 1126-1167.

[22] Ravera, S.; Bartolucci, M.; Cuccarolo, P.; Litamè, E.; Illarcio, M.; Calzia, D.; Degan, P.; Morelli, A.; Panfoli, I. Oxidative stress in myelin sheath: The other face of the extramitochondrial oxidative phosphorylation ability. *Free Radic. Res.* 2015, *49*, 1156-64.

[23] Higuera-Ciapara, I.; Félix-Valenzuela, L.; Goycoolea, F.M. Astaxanthin: A review of its chemistry and applications. Crit Rev *Food Sci. Nutr.* 2006, *46*, 185-196.

[24] Ambati, R.R.; Phang, S.M.; Ravi, S.; Aswathanarayana, R.G. Astaxanthin: Sources, extraction, stability, biological activities and its commercial applications—a review. *Mar Drugs* 2014, *12*, 128-52.

[25] Kim, S.H.; Lim, J.W.; Kim, H. Astaxanthin Inhibits Mitochondrial Dysfunction and Interleukin-8 Expression in Helicobacter pylori-Infected Gastric Epithelial Cells. *Nutrients* 2018, *10*, 1320.

[26] Song, X.; Wang, B.; Lin, S.; Jing, L.; Mao, C.; Xu, P.; Lv, C.; Liu, W.; Zuo, J. Astaxanthin inhibits apoptosis in alveolar epithelial cells type II in vivo and in vitro through the ROS-dependent mitochondrial signalling pathway. *J. Cell Mol. Med.* 2014, *18*, 2198-212.

[27] Chen, Y.; Li, S.; Guo, Y.; Yu, H.; Bao, Y.; Xin, X.; Yang, H.; Ni, X.; Wu, N.; Jia, D. Astaxanthin Attenuates Hypertensive Vascular Remodeling by Protecting Vascular Smooth Muscle Cells from Oxidative Stress-Induced Mitochondrial Dysfunction. *Oxid. Med. Cell Longev.* 2020, *2020*, 4629189.

[28] Yin, M.; O'Neill, L.A.J. The role of the electron transport chain in immunity. *FASEB. J.* 2021, *35(12)*, e21974.

[29] Brand, M.D. Mitochondrial generation of superoxide and hydrogen peroxide as the source of mitochondrial redox signaling. *Free Radic. Biol. Med.* 2016, *100*, 14-31.

[30] Goncalves, R.L.; Quinlan, C.L.; Perevoshchikova, I.V.; Hey-Mogensen, M.; Brand, M.D. Sites of superoxide and hydrogen peroxide production by muscle mitochondria assessed ex vivo under conditions mimicking rest and exercise. *J. Biol. Chem.* 2015, *290*, 209-27.

[31] Chouchani, E.T.; Pell, V.R.; Gaude, E.; Work, L.M.; Frezza, C.; Krieg, T.; Murphy, M.P.; et al. Ischaemic accumulation of succinate controls reperfusion injury through mitochondrial ROS. *Nature* 2014, *515*, 431-435.

[32] Scialò, F.; Sriram, A.; Fernández-Ayala, D.; Gubina, N.; Lõhmus, M.; Nelson, G.; Logan, A.; Cooper, H.M.; Navas, P.; Enríquez, J.A.; Murphy, M.P.; Sanz, A. Mitochondrial ROS

Produced via Reverse Electron Transport Extend Animal Lifespan. *Cell. Metab.* 2016, 23(4), 725-34.

[33] Scialò, F.; Fernández-Ayala, D.J.; Sanz, A. Role of Mitochondrial Reverse Electron Transport in ROS Signaling: Potential Roles in Health and Disease. *Front Physiol.* 2017, 8, 428.

[34] Aki, T.; Funakoshi, T.; Noritake, K.; Unuma, K.; Uemura, K. Extracellular glucose is crucially involved in the fate decision of LPS-stimulated RAW264.7 murine macrophage cells. *Sci. Rep.* 2020, 10(1), 10581.

[35] Murphy, M.P. How mitochondria produce reactive oxygen species. *Biochem. J.* 2009, 417(1), 1-13.

[36] Mills, E.L.; Kelly, B.; Logan, A.; Frezza, C.; Murphy, M.P.; O'Neill, L.A.; et al. Succinate Dehydrogenase Supports Metabolic Repurposing of Mitochondria to Drive Inflammatory Macrophages. *Cell* 2016, *167*, 457-470

[37] Kelly, B.; Tannahill, G.M.; Murphy, M.P.; O'Neill, L.A. Metformin Inhibits the Production of Reactive Oxygen Species from NADH: Ubiquinone Oxidoreductase to Limit Induction of Interleukin-1β (IL-1β) and Boosts Interleukin-10 (IL-10) in Lipopolysaccharide (LPS)-activated Macrophages. *J. Biol. Chem.* 2015, *290*, 20348-59.

[38] Hederstedt, L.; Rutberg, L. Succinate dehydrogenase--a comparative review. *Microbiol. Rev.* 1981, *45*, 542-55.

[39] Moreno, C.; Santos, R.M.; Burns, R.; Zhang, W.C. Succinate Dehydrogenase and Ribonucleic Acid Networks in Cancer and Other Diseases. *Cancers (Basel)* 2020, *12*, 3237.

[40] Nastasi, C.; Willerlev-Olsen, A.; Dalhoff, K.; Ford, S.L.; Gadsbøll, A.Ø.; Buus, T.B.; Gluud, M.; Danielsen, M.; Litman, T.; Bonefeld, C.M.; Geisler, C.; Ødum, N.; Woetmann, A. Inhibition of succinate dehydrogenase activity impairs human T cell activation and function. *Sci. Rep.* 2021, *11*, 1458.

[41] Garaude, J.; Acín-Pérez, R.; Martínez-Cano, S.; Enamorado, M.; Ugolini, M.; Nistal-Villán, E.; Hervás-Stubbs, S.; Pelegrín, P.; Sander, L.E.; Enríquez, J.A.; Sancho, D. Mitochondrial respiratory-chain adaptations in macrophages contribute to antibacterial host defense. *Nat. Immunol.* 2016, *17*, 1037-1045.

[42] Mills, E.; O'Neill, L.A. Succinate: a metabolic signal in inflammation. *Trends Cell Biol.* 2014, *24*, 313-20.

[43] Murphy, M.P.; O'Neill, L.A.J. Krebs Cycle Reimagined: The Emerging Roles of Succinate and Itaconate as Signal Transducers. *Cell* 2018, *174*, 780-784.

[44] Brand, M.D. The sites and topology of mitochondrial superoxide production. *Exp. Gerontol.* 2010, *45*, 466-472.

[45] Ryan, D.G.; O'Neill, L.A.J. Krebs Cycle Reborn in Macrophage Immunometabolism. *Annu. Rev. Immunol.* 2020, *38*, 289-313.

[46] McGettrick, A.F.; O'Neill, L.A.J. The Role of HIF in Immunity and Inflammation. *Cell Metab.* 2020, *32*, 524-536.

[47] Murdoch, C.; Muthana, M.; Lewis, C.E. Hypoxia regulates macrophage functions in inflammation. *J. Immunol.* 2005, *175*, 6257-63.

[48] Blouin, C.C.; Pagé, E.L.; Soucy, G.M.; Richard, D.E. Hypoxic gene activation by lipopolysaccharide in macrophages: implication of hypoxia-inducible factor 1alpha. *Blood* 2004, *103*, 1124-1130.

[49] Mi, Z.; Rapisarda, A.; Taylor, L.; Brooks, A.; Creighton-Gutteridge, M.; Melillo, G.; Varesio, L. Synergystic induction of HIF-1alpha transcriptional activity by hypoxia and lipopolysaccharide in macrophages. *Cell Cycle* 2008, *7*, 232-41.

[50] Takeda, N.; O'Dea, E.L.; Doedens, A.; Kim, J.W.; Weidemann, A.; Stockmann, C.; Asagiri, M.; Simon, M.C.; Hoffmann, A.; Johnson, R.S. Differential activation and antagonistic function of HIF-{alpha} isoforms in macrophages are essential for NO homeostasis. *Genes Dev.* 2010, *24*, 491-501.

[51] Fuhrmann, D.C.; Wittig, I.; Brüne, B. TMEM126B deficiency reduces mitochondrial SDH oxidation by LPS, attenuating HIF-1α stabilization and IL-1β expression. *Redox Biol.* 2019, *20*, 204-216.

[52] Guzy, R.D.; Sharma, B.; Bell, E.; Chandel, N.S.; Schumacker, P.T. Loss of the SdhB, but Not the SdhA, subunit of complex II triggers reactive oxygen species-dependent hypoxia-inducible factor activation and tumorigenesis. *Mol. Cell. Biol.* 2008, *28*, 718-31.

[53] Ainscow, E.K.; Brand, M.D. Internal regulation of ATP turnover, glycolysis and oxidative phosphorylation in rat hepatocytes. *Eur. J. Biochem.* 1999, *266*, 737-49.

[54] Selak, M.A.; Armour, S.M.; MacKenzie, E.D.; Boulahbel, H. Watson, D.G.; Mansfield, K.D.; Pan, Y.; Simon, M.C.; Thompson, C.B.; Gottlieb, E. Succinate links TCA cycle dysfunction to oncogenesis by inhibiting HIF-alpha prolyl hydroxylase. *Cancer Cell* 2005, *7*, 77-85.

[55] Taylor, C.T.; Scholz, C.C. The effect of HIF on metabolism and immunity. *Nat. Rev. Nephrol.* 2022, *18*, 573-587.

[56] Corcoran, S.E.; O'Neill, L.A. HIF1α and metabolic reprogramming in inflammation. *J. Clin. Invest.* 2016, *126*, 3699-3707.

Abbreviations

AA5	Atpenin A5
AnA	antimycinA
ATP	adenosine triphosphate
AX	astasxanthin
BCA	bicinchoninic acid
DMEM	Dulbecco's modified Eagle medium
DMSO	dimethyl sulfoxide
DNA	deoxyribonucleic acid
ECAR	extracellular acidification rate
EDTA	ethylenediaminetetraacetic acid
ELISA	enzyme-linked immunosorbent assay
ETC	electron transport chain
FBS	fetal bovine serum
FCCP	carbonyl cyanide 4-trifluoromethoxy phenylhydrazone
HBSS	Hank's balanced salt solutions
HIF-1α	hypoxia-inducible factor-1α
IL	interleukin
iNOS	inducible nitric oxide synthase
LPS	lipopolysaccharides
MCP	monocyte chemoattractant protein
MMP	mitochondrial membrane potential
mtDNA	mitochondrial DNA
mtROS	mitochondrial reactive oxygen species
NADH	nicotinamide adenine dinucleotide
OCR	oxygen consumption rate
OXPHOS	oxidative phosphorylation
PBS	phosphate buffered saline
qRT-PCR	quantitative real-time polymerase chain reaction
ROS	reactive oxygen species
Rot	rotenone
SDH	succinate dehydrogenase
Sdhb	succinate dehydrogenase complex, subunit B
TCA	tricarboxylic acid
TNF	tumor necrosis factor
2-DG	2-deoxy-glucose

Chapter IV General Conclusion

Globally, the proportion of people over 65 years of age to the total population (the aging rate) is increasing, and aging is expected to grow rapidly not only in developed regions where it is already occurring, but also in developing regions. It is well known that physical functions decline with age (aging). In addition, age-related diseases such as atherosclerosis (cardiovascular disease), diabetes (metabolic disorders), sarcopenia (muscle aging and dysfunction), Alzheimer's diseases (brain aging and neurodegenerative disease), macular degeneration (eye disease) are increasingly associated with the aging process as we age. Several studies in model organisms and humans over the past decades have reported that mitochondrial function plays an important role in the aging process. Mitochondrial dysfunction leads to the accumulation of chronic oxidative stress and age-related diseases. Therefore, maintaining mitochondrial function may help the prevention of age-related diseases. AX, a marine carotenoid found in the epidermis of microalgae, yeast, crustaceans and fish, has been shown to have many functions, including antioxidant, anti-inflammatory and anti-fatigue effects. Among these, its role in scavenging ROS (antioxidant effect) is widely known, and it has been reported to show 6000 times more antioxidant capacity compared to vitamin c. It has been suggested that this is due to the fact that AX has hydrophobic and hydrophilic groups in its structure, which allows itself to penetrate cell membranes and effectively exert its antioxidant capacity. Interestingly, AX has been reported to accumulate relatively easily in mitochondria, which have a similar phospholipid bilayer membrane structure to cell membranes. In the doctoral research, I focused on the effects of marine carotenoid AX on two typical age-related diseases, muscle atrophy and immune disorders, both of which are caused by mitochondrial dysfunction and metabolic disorders.

In Chapter II, the effects of AX on mitochondria in skeletal muscle and the effects of AX on muscle atrophy induced by mitochondrial damage were investigated. C57BL/6J mice were fed a normal diet or an AX diet formulated at 0.2% by weight (0.02%AX) for 4weeks, and tail suspension was performed for 2 weeks to establish a muscle-atrophied mouse model. The effects of AX were evaluated by *in vivo* model. In addition, the mechanism of action of AX in mitochondria was examined using Sol8 myotubes derived from SO muscle *in vitro* model. In the normal diet group, tail suspension resulted in a decrease in muscle weight. In contrast, the soleus muscle, which consists mostly of type I slow-twitch and type IIa intermediate muscle fibers, showed no reduction in muscle weight or cross-sectional area of muscle fibers in the AX diet group, even when a muscle atrophy model was applied. Furthermore, the AX diet group significantly inhibited the production of mitochondria-derived ROS and the decrease in mitochondrial respiratory chain complex protein content induced by tail suspension. In addition, the expression levels of mitochondrial biosynthesis synthesis genes such as *AMPK α-1, PPAR-γ, and Ckmt 2* impaired by muscle atrophy were improved by AX. To confirm the AX phenotype in the SO muscle, we examined its effects on mitochondria using Sol8 myotubes derived from the SO muscle. AX was preferentially detected in the mitochondrial fraction, it significantly suppressed the production of mitochondrial respiratory chain complex III-derived ROS and ameliorated the decrease in MMP caused by mitochondrial respiratory chain complex damage. Moreover, AX inhibited the activation of caspase 3 via inhibiting the release of cytochrome c into the cytosol in AnA-treated Sol8 myotubes. These results suggested that AX protected the functional stability of mitochondria, alleviated mitochondrial oxidative stress and

mitochondria-mediated apoptosis, and thus, prevented age-related muscle atrophy which caused by mitochondrial oxidative stress and dysfunction.

In Chapter III, The mouse macrophage-like cell line RAW264.7 cells were used to investigate the effects of AX on immune disorders induced by mitochondrial dysfunction. Although AX has been shown to have anti-inflammatory effects in various cells, the mechanisms are quite different. In particular, the role of AX on mitochondrial metabolism in macrophages are still unknown. In this part, RAW264.7 cells were stimulated with LPS, establishing a classical inflammation model. Then, the mitochondria-mediated inflammation and its mechanisms were investigated. LPS stimulation significantly increased the expression and secretion of the proinflammatory cytokine IL-1β. In contrast, AX-treated cells significantly suppressed IL-1β production. Additionally, AX attenuated the mitochondrial O_2^- production and maintained the mitochondrial membrane potential, implying that AX preserved mitochondrial homeostasis to avoid LPS stimulation-induced mitochondrial dysfunction. Moreover, AX prevented the decrease of mitochondrial complexes I, II, and III, which caused by LPS stimulation. Especially, AX inhibited the reduction of mitochondrial succinate dehydrogenase (SDH; complex II) activity and upregulated the protein and mRNA level of SDH complex, subunit B. Furthermore, analysis by using AA5, an inhibitor of SDH, revealed that AX directly acts on mitochondria upstream of the SDH-HIF-1α signaling pathway and inhibits IL-1β expression. To explore whether the effect of AX are involved in mitochondrial metabolism, the intracellular energy metabolim are measured. LPS stimulation caused cells to exhibit glycolytic-dependent energy metabolism, whereas AX-treated cells showed oxidative phosphorylation-dependent energy metabolism. These findings revealed important effects of

AX on mitochondrial metabolism enzymes as well as on mitochondrial energy metabolism in the immune response. In addition, these raised the possibility that AX plays an important role in other diseases caused by mitochondrial SDH mutation and mitochodrial metabolic disorders.

In summary, a protective effect of AX on mitochondrial function: it plays a regulatory role in mitochondrial respiratory complex expression, transcription factors and energy metabolism. All these play a vital role in diseases of aging (the graphical summary shown as Fig. 4-1). These results also suggested that the potential effect of AX on other diseases related to mitochondrial dysfunction and metabolic disorders. Clinicians strive to provide answers to their patients, but there are many unanswered questions related to the role of nutrition on disease prevention [1-3]. Therefore, it is necessary and important to explore the biological activity of different nutrients. In today's rapidly aging society, dietary AX supplements would reduce the incidence of age-related diseases and delay the aging process, extending human lifespan. Furthermore, based on the unique structure of AX and the existing base of inquiry, in future studies, other biological activities of AX and the mechanisms of action in different signaling pathway still need to be investigated. In addition, the cross-talk between the role of AX in different mechanisms and different kinds of age-related diseases will also be gradually explored.

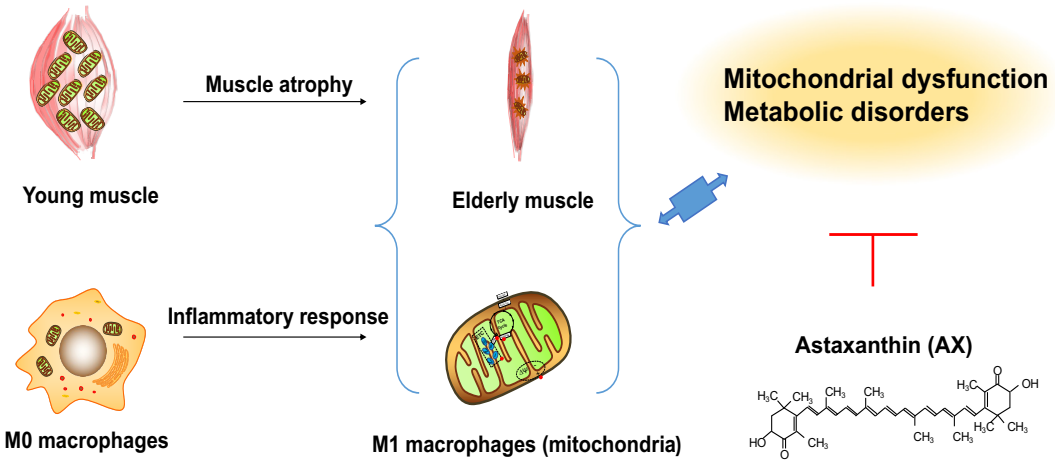

Figure 4-1. The summary of the effect of AX on age-related muscle atrophy and inflammation which caused by mitochondrial dysfunction and metabolic disorders.

References

[1] Fleischer, D.M.; Spergel, J.M.; Assa'ad, A.H.; Pongracic, J.A. Primary prevention of allergic disease through nutritional interventions. *J. Allergy Clin. Immunol. Pract.* 2013, *1*, 29-36.

[2] Muraro, A.; Halken, S.; Arshad, S.H.; Beyer, K.; Dubois, A.E.; DuToit,G.; Eigenmann, P.A.; Grimshaw, K.E.; Hoest, A.; Lack, G.; et al. EAACI food allergy and anaphylaxis guidelines. Primary prevention of food allergy. *Allergy* 2014, *69*, 590-601.

[3] Venter, C.; Eyerich, S.; Sarin, T.; Klatt, K.C. Nutrition and the Immune System: A Complicated Tango. *Nutrients* 2020, *12*, 818.

Acknowledgments

I would like to express my deepest gratitude and sincere thanks to the flowing:

Assoc. Prof. Katsuya Hirasaka (Graduate School of Fisheries and Environmental Sciences, Nagasaki University), my supervisor, for accepting me in his laboratory, advising me experiments, giving me the opportunities and platform, taking care of my living while I have been in Japan；

Prof. Kiyoshi Osatomi (Graduate School of Fisheries and Environmental Sciences, Nagasaki University), Prof. Kenichi Yamaguchi (Graduate School of Fisheries and Environmental Sciences, Nagasaki University), Assoc. Prof. Asami Yoshida (Graduate School of Fisheries and Environmental Sciences, Nagasaki University) for their valuable and constructive comments and suggestions to my thesis and presentation;

Assoc. Prof. Ryoichi Mori (Department of Pathology, Graduate School of Biomedical Sciences, Nagasaki University), Dr. Sangeun Kim (Department of Investigative Pathology, Graduate School of Biomedical Sciences, Nagasaki University) for their patient guidance and help and great contribution to my doctoral research especially Chapter III;

Prof. Katsuyasu Tachibana (Graduate School of Fisheries and Environmental Sciences, Nagasaki University), Prof. Shigeto Taniyama (Graduate School of Fisheries and Environmental Sciences, Nagasaki University) for giving advices to my research;

Nobuyuki Miyaji (Toyo Koso Kagaku Co., Ltd., Chiba) for providing the experimental materials;

All the students under the supervision of Assoc. Prof. Katsuya Hirasaka from April 2018 to March 2023 and classmates for all the help;

Nagasaki University WISE (“Doctoral Programme for World-leading Innovative and Smart Education” for Global Health) Programme, for the platform and financial support to my life and my research;

My family especially my parents, my friends, for all the love and support;

Everyone I have met. Although everyone has different personalities and different perspectives, meeting is fate and luck.